NTNU

Norwegian University of
Science and Technology

Analysis and Prediction of Gas Lift Stability from Field Data

Eivind Litland Myhr

Petroleum Geoscience and Engineering
Submission date: June 2017
Supervisor: Harald Arne Asheim, IGP

Norwegian University of Science and Technology
Department of Geoscience and Petroleum

Preface

This Master's thesis is the final work of the Master of Science degree in Petroleum Production Engineering, at the Department of Geoscience and Petroleum at the Norwegian University of Science and Technology (NTNU) in Trondheim, Norway.

First and foremost, I would like to thank my supervisor, Professor Harald Arne Asheim for his inspirational guidance and for providing me with the model used in the thesis. This is much appreciated. I would also like to thank Statoil ASA (operator of the Heidrun field) for providing the field data. The view expressed in this paper are the views of the author and do not necessarily reflect the views of Statoil ASA.

Thank you to all my friends and fellow students.

Thank you to Helene, for all her support.

Lastly, I would like to thank my family for all their support and encouragement throughout my years at NTNU.

Eivind Litland Myhr
Trondheim, June 2017

Abstract

Producing oil wells on continuous gas lift may under certain operating conditions develop flow instabilities. Prediction on beforehand may enable prevention by design and operational changes. Stability criteria exist, but gas lift wells predicted stable by such criteria often turn out unstable in practice.

A theoretical gas lift model has been tested against field data and the stability of a gas lift well investigated. Based on existing stability criteria, the new model pretends to improve the prediction power by considering the outflow variations explicitly. Incorporating the outflow in the model is physically reasonable and seems to improve prediction capabilities in certain cases. Dynamic production characteristics in the well have been explored in detail, and the model response compared with measured dynamics. The dynamic response of the model is predicted using numerical simulation as well as an analytical solution.

Analysis of the data showed the well might develop severe oscillations. These appear to be initiated by the combination of varying density of the produced fluid mixture and disturbances in the gas delivery system. The proposed model predicts the well stable for all stationary production periods examined. In periods of flow instability in field data, the model prediction is in disagreement with observed response.

A parametric sensitivity study has been performed and demonstrated the model is capable of capturing the effect of main design and reservoir parameters on stability. When the outflow response is excluded from the model, the prediction capabilities seems to be reduced.

Abstrakt

Oljebrønner som produserer ved kontinuerlig gassløft kan ved enkelte driftsforhold utvikle strømningsustabiliteter som forstyrrer produksjonen. Prediksjon av ustabilitet på forhånd er ønskelig, og kan hindre ustabilitet ved hjelp av drifts- og designendringer. Ulike stabilitetskriterier eksisterer, men gassløftbrønner predikert stabile ved slike kriterier viser seg ofte å være ustabile i praksis.

En teoretisk gassløftmodell har blitt testet mot feltdata og stabiliteten av en gassløftet brønn har blitt undersøkt. Den teoretiske modellen forsøker å forbedre prediksjonen av stabilitet ved å inkludere variasjonene ved utløpet av produksjonsrøret. Hovedforskjellen mellom den nye modellen og eksisterende kriterier og tilnærminger er at variasjonen ved utløpet er inkludert. Dette ser ut til å forbedre modellens prediksjonsevner i enkelte tilfeller.

Feltmålingene viser at brønnen klarer å opprettholde stabil produksjon bare i kortere perioder før produksjonen utvikler alvorlig strømningsustabilitet. Analysen antyder at ustabiliteten skyldes kombinasjonen av varierende tetthet av den produserte fluidblandingen og forstyrrelser i gassleveransesystemet. Basert på feltmålingene predikerer den nye modellen brønnen stabil i alle stasjonære produksjonsperioder som er undersøkt. I perioder med klar strømningsustabilitet stemmer ikke modellens forutsigelser med oppførselen observert fra feltmålingene.

En parametrisk simuleringsstudie er utført og viser modellen er i stand til å vurdere effekten av viktige design- og reservoarparametere på stabilitet. Når variasjonene ved utløpet av produksjonsrøret er ekskludert ser det ut til at modellens prediksjonsevner er redusert.

Contents

List of Figures

List of Tables

Chapter 1

Introduction

1.1 Motivation

In the specialization project in the autumn of 2016, the author investigated the stability of a gas lift well in the Norwegian Sea. The analysis was based on existing criteria and showed strong disagreement between predicted and measured well response. This thesis is a continuation of the work and is intended to check a new gas lift model. The suggested model is a simplification, and thus its applicability needs to be checked against measurements.

Field data have been provided, and this gives the opportunity to investigate the actual dynamics in the well under specific operating conditions and enables the model response to be compared with measurements. Utilizing the model aspects of instability will be studied and compared with existing theories and standards. The model builds upon existing criteria but includes some modifications that hopefully will improve prediction of stability in gas lift wells.

1.2 Outline

The report is divided into ten chapters. Chapter 2 gives a short introduction to the gas lift method and the main components of the system. Chapter 3 provides the basic principles of instability and describe the different types of flow instability in gas lift wells. The consequences of unstable production will also be outlined in this section. Chapter 4 addresses selected stability theories from literature while Chapter 5 discuss the implementation of active control systems in gas lift wells. The part on stability theory include both analytical criteria and graphical solutions to predict the onset of instability. The theory discussed in Chapters 2-5 is partly based on the author‘s previous project work (Myhr, 2016).

Chapter 6 form the theoretical basis for the new gas lift model to be tested against field data. The model itself and the assumptions behind it are presented in detail and compared against existing criteria. Chapter 7 accommodate the in-depth stability analysis of the well

in the Heidrun field and provide the operational basis for the proposed gas lift model. Chapter 8 examines the gas lift model by checking it against the field measurements. Numerical simulation explores the theoretical model against the data. Also, its prediction power and the dynamical response is tested and checked with an analytical solution.

Chapter 9 summarizes the most significant findings from the stability study and the model test results. Possible causes for instability in the Heidrun well are discussed, and the prediction power of the gas lift model are explained. Model results that differ from field data or existing theories are highlighted in this section. Lastly, Chapter 10 concludes the results of the field data analysis and model test results, based on the discussion in Chapter 9.

Chapter 2

The gas lift system

In traditional gas lift systems, gas lift is accomplished by injecting gas at high pressure through the wellhead and down into the annular volume between the tubing and casing. The compressed gas mixture enters the production tubing through an orifice valve and mixes with the flowing fluid in the tubing. The injection of gas to the tubing lowers the density of the flowing fluid mixture in the tubing and reduces the hydrostatic pressure gradient in the well accordingly. Figure 2.0.1 shows a simplified setup of a gas lift well and the main components.

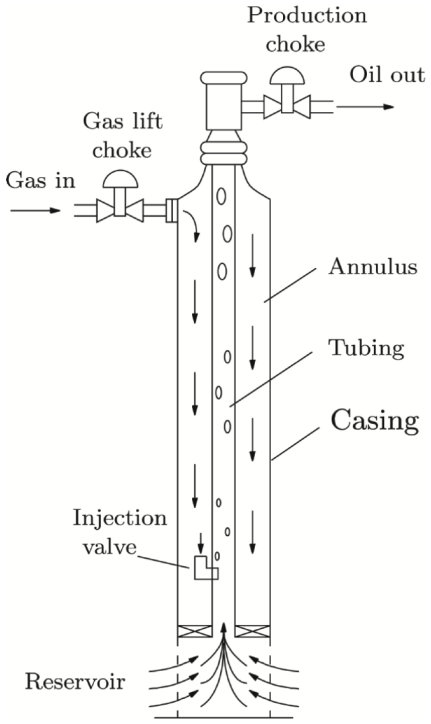

Figure 2.0.1: The gas lift system and main components (Eikrem et al., 2008).

Injection valves provide communication between annulus and tubing. The size is selected such that the pressure drop across the valve is an approximately 3-6 bar for a given gas injection rate (Fairuzov et al., 2004).

The injection valve usually comprises an orifice port and a check valve. Proper sizing of the injection orifice ensures a steady inflow of lift-gas while a check valve prevents the influx of reservoir fluid from the tubing to the annulus (Bellarby, 2009).

Poettman et al. (1952) and Bertuzzi et al. (1953) proposed design principles that are still valid. The design principles are used to verify the gas lift design and relate the gas injection rate and associated oil rate and may be used to obtain the optimum combination of flow rates. An efficient and functional gas lift system is important for various reasons. Too high injection rate may both reduce oil production and increase the overall costs of the operation (Poettman and Carpenter, 1952; Bertuzzi et al., 1953).

Injection of lift-gas increase the flow rate in the production tubing and will cause increased frictional pressure drop. To obtain an efficient gas lift design, it is necessary to compare the reduction in hydrostatic pressure and the increased frictional pressure drop.

For a gravity dominated system gas lift may be favorable and increasing the injection rate may improve oil production. In the event of a well dominated by frictional pressure drop, i.e. high gas-oil ratio, the benefit of gas lift is usually lower. In fact, under certain conditions, the method may be counterproductive, and other artificial lift methods should be considered. When too much gas is flowing in the tubing, the injection of lift-gas may cause phase slippage. When slippage occurs, the frictional pressure drop overcomes the hydrostatic pressure drop in the well, and less energy is available to transport the liquid along the production tubing.

Thus gas lift should preferably be considered as an artificial lift method in wells producing heavy oils with low gas content or in wells with high water cut. (Saepudin et al., 2007).

Chapter 3

Gas lift instability

Gas lift systems comprise multiphase flow of oil and gas, and usually also water. Nearly all multiphase flow systems experience rate and pressure variations because of redistribution of gas and liquids. The variations cause relatively small flow changes with short durations. By itself, this has little effect on production. In gas lifted wells, however, it may bring about flow instabilities (Avest and Oudeman, 1995).

3.1 Hydrodynamic slugging

Hydrodynamic slugging denote instability that occurs on the gas-liquid interface in the flowing fluid mixture. These variations may be described as a discontinuous redistribution of fluids and may cause small density and pressure changes in the production tubing (Liu and Vandu, 2005). Hydrodynamic slugging is natural occurring in gas lift systems and is usually not considered a problem to production (Asheim, 1988).

3.2 System instability

System instability denotes variations that comprise the entire gas lift production system, often as cyclic variations of large amplitudes. These may cause operational problems in the production facilities and decreases the efficiency of the gas lift system (Alhanati et al., 1993).

Gang and Golan (1989) claimed system instability has a systematic background and are caused by the inertia and feedback effects of the gas lift system. When such instability is experienced, the system continues to oscillate about an average level periodically.

Two types of system instability are reported in the literature, casing heading and tubing heading instability.

3.2.1 Casing heading

By casing heading is understood instability that involves pressure variations in the annulus, detectable at the casing head. Gilbert (1954) described casing heading in flowing oil wells and claimed that it could be suppressed by installing packers. Since then, casing heading has been the subject of several studies (Asheim, 1988; Gang and Golan, 1989; Blick et al., 1988; Alhanati et al., 1993).

Casing heading develops in the system as result of communication between the production tubing and annulus at the injection valve. The communication between tubing depends on the characteristics of the valve. Thus the valve has a significant impact on how changes in the tubing influence the annulus. In continuous gas lift wells, heading may be observed if the flow through the injection valve is sub-critical. Under this condition, the injection rate depends on the downstream tubing pressure. At critical flow, however, any changes of the condition in the production tubing will not affect the injection rate (Hu and Golan, 2003).

By traditional gas lift design, constant inflow of lift-gas to the tubing is assumed. The pressure in the production tubing may exhibit temporary variations, causing temporary variations in the inflow of lift-gas. By casing heading, an increase in the inflow of gas leads to increased pressure difference between the annulus and the production tubing. This causes the inflow of lift-gas to increase further, and this positive feedback causes the well to exhibit unstable flow behavior. However, if an increased inflow of lift-gas causes decreased pressure difference across the annulus and tubing the inflow of lift-gas will decrease. In this case, the system is stabilized by negative feedback (Asheim, 1988).

The mechanism above may also be described analytically by considering the flow equations in the annulus and production tubing. By looking at incremental changes in flow rate and pressure, it is possible to investigate the response of the system away from its steady-state solution. In many cases, the well opposes the disturbances and have a dampening response to small changes, which is called negative feedback. In some situations, however, the response of the gas lift system may amplify the disturbances and flow instabilities may develop (Gang and Golan, 1989).

3.2.2 Tubing heading

By tubing heading is understood instability that does not involve annulus pressure variations, thus without variation of the gas injection rate. This is a rather new phenomenon discovered in gas lift wells in the North Sea, producing from depleted reservoirs. Unlike casing heading, the tubing heading instability may develop in gas lift wells in which the inflow of lift gas is critical (Hu and Golan, 2003).

When the inflow of lift-gas is constant, any variation to the liquid inflow from the reservoir results in a density change in the fluid mixture at the bottom of the well. The density of the fluid mixture will vary due to variation to the phase fractions. The density change will travel along the tubing as density wave and reach the exit of the tubing after a period of time. This generates a small change to the pressure drop in the tubing and will affect the inflow to the wellbore.

Hu and Golan (2003) claimed that the occurrence of tubing heading does not necessary shift the gas lift system to become unstable since the well has a self-controlling effect. This means that any decrease in the pressure drop due to decreased mixture density results in an increase of the liquid inflow from the reservoir, and opposite. However, this mechanism is out of phase due to the delay between the inflow and outflow in the production tubing. Under certain conditions, the self-controlling mechanism might break down and the well exhibit flow instabilities (Hu and Golan, 2003).

3.3 Consequences of instability

Instability in continuous gas lift wells has several disadvantages. Operating under cyclic conditions are associated with operational issues like unplanned shutdowns and increased maintenance. Periods of reduced liquid production followed by large plugs of gas and liquid may result in poor separation and limit the separator capacity (Slupphaug and Bjune, 2006). Also, periods of very high gas rates may lead to excessive flaring. Pressure surges and rate variation in the production facilities are associated with production control, gas allocation, and can prevent reliable production measurements and well tests. The variations, in turn, can make it difficult to predict future production and the storage and transportation needed (Alhanati et al., 1993).

Beside operational problems, Hu and Golan (2003) pointed out production loss as another important consequence of unstable gas lift wells. The authors simulated the production loss due to casing heading and claimed that up to 35 % production loss could be expected. Guerrero-Sarabia and Fairuzov (2013) did a similar study and discovered a reduction in oil production of 27 %. Thus, to reach the desired recovery from the field/well the tail production must be prolonged to compensate for the reduced production rates. This may increase the costs of the project due to the extended ongoing operational costs. The overall consequence of unstable production is safety and profit-reducing issues and reduced efficiency of the gas lift system (Hu and Golan, 2003).

Chapter 4

Stability theory

4.1 Early observations

Since early 1950, numerous studies on instability in gas lift wells have been reported. Among them, the first comprehensive study of instability was given by Gilbert (1954).

In his study, Gilbert made observations and characterized the instability processes in naturally flowing oil wells completed without production packers. Gilbert observed that associated gas could accumulate in the annulus. The accumulation initiated flow instabilities when the gas in the annulus reached sufficiently high pressure and started to flow into the tubing. The accumulation of gas in annulus changed the rate and pressure conditions in the well. Gilbert claimed instability could be eliminated by the use of packers between the production casing and tubing.

In wells already producing, Gilbert suggested installing pressure actuated valves. At a preset lower annulus pressure the tubing outlet choke will close such that reservoir fluids flow into the annulus and accumulate. The influx of reservoir fluids will cause a rapid pressure increase in the annulus, after which the valve is opened at a given maximum pressure (Gilbert, 1954). According to Gilbert, this mechanism could eliminate instability in oil wells completed without packer. Today, however, all wells are equipped with packers and this eliminates the need for valves of this type in the production tubing.

Bertuzzi et al. (1953) described the mechanism of heading in gas lift wells and observed that heading would occur if the injection rate were reduced below a certain minimum. In the event of severe heading, the liquid production would eventually stop. They claimed that a drop in the tubing pressure brought about a sudden flow of gas into the tubing. The amount of gas flowing into the tubing depends on the volume and the pressure in the annulus. If the annular pressure dropped too much, gas stopped to flow into the production tubing (Bertuzzi et al., 1953).

Several attempts have been made to understand and quantify flow instability in gas lift wells with numerical approaches and techniques, similar to what Grupping et al. (1984) did. They succeeded in demonstrating instability by numerical means and suggested stabilizing measures for gas lift wells (Grupping et al., 1984). Fitremann and Vedrines (1985) performed linear stability analysis on a mathematical model of a gas lift system. The results were shown to resemble small-scale laboratory experiments. No comparisons with field data were attempted (Fitremann and Vedrines, 1985).

4.2 Asheim

As a simplification of Fitremann's analysis, Asheim (1988) developed two explicit criteria for stability in gas lift wells. The criteria are derived by considering how the gas lift system, initially in equilibrium, respond small changes in the well conditions.

The derivation is based on how the injection system and reservoir respond to a change in the tubing pressure. Transient inflow is neglected, and the relationship between the well pressure and flow from the reservoir is assumed to be described by the steady-state inflow relationship. Grupping et al. (1984) and Fitremann and Vedrines (1985) did the same assumption in their study. Furthermore, slippage is neglected, and the flow through the gas lift valve assumed isothermal and incompressible. The system is considered gravity dominated, and acceleration and frictional forces are disregarded.

Inflow response

The first criterion quantifies stability as a consequence of the inflow responses of injection gas and reservoir fluid inflow. The inflow from the reservoir acts stabilizing because it introduces heavier fluids into the production tubing. If the inflow of reservoir fluid is more sensitive to pressure than the gas injection rate, the density of the fluids in the production tubing will increase. The inflow causes an increase in the pressure in the tubing and has a stabilizing effect on the system. Stabilization by the inflow response is given as

$$F_1 = \frac{\rho_{gsc} B_g q_{gsc}^2}{q_{Lsc}} \frac{J}{(EA_i)^2} > 1. \tag{4.2.1}$$

By equation 4.2.1, stability is favored by a high inflow rate of lift-gas, small injection port size, and high productivity index. Also, criterion F_1 show a high density of the lift-gas is stabilizing. However, the gas density is in general low compared to the liquid density.

Depletion response

If equation 4.2.1 is not satisfied, a decrease in the pressure in the tubing will cause the inflow of lift-gas to increase more than the liquid rate from the reservoir. The increased inflow of gas will deplete the pressure in the annulus and decrease the tubing pressure. If the pressure in the annulus depletes faster than the pressure in the tubing, then the pressure difference between the tubing and annulus will decrease. This reduces the inflow of lift-gas, and stabilizes the system. Stabilization by the pressure-depletion response is given as

$$F_2 = \frac{V_t}{V_c}\frac{1}{gD}\frac{p_{ti}}{(\rho_{fi}-\rho_{gi})}\frac{q_{fi}+q_{gi}}{q_{fi}(1-F_1)} > 1. \tag{4.2.2}$$

By equation 4.2.2, stability is stimulated by a high inflow rate of lift-gas and a small volume of the annulus. While confirming that a high injection rate is beneficial the inequality also shows that a high tubing pressure is stabilizing.

4.3 Blick et al.

Blick et al. (1988) approached the stability problem differently than Asheim. They developed a mathematical model consisting of differential equations describing the transient responses in a gas lift system. The purpose of the model was to analyze the influence of small variations from the steady-state of the injection rate, pressure at the injection point, and the reservoir inflow. The differential equations are Laplace transformed and then combined by Cramer‘s rule to obtain the solutions as a linear system of equations. The procedure produces a characteristic equation with three coefficients, and the model predicts the gas lift system stable when the coefficients are all positive or negative. If one of the coefficients have a sign that is different, the well is predicted unstable and small flow perturbations increase with time. Blick et al. used their model on hypothetical gas lift wells but never compared the result with any field data (Blick et al., 1988).

4.4 Gang and Golan

Gang and Golan (1989) worked out a criterion for assuring smooth and stable operation of gas lift wells. The purpose of the study was to aid the design of continuous gas lift wells by giving recommendations on the selection and settings of the production choke, downhole gas lift ori-

fice, and injection choke (Gang and Golan, 1989). Two types of instabilities are addressed in the study, static and dynamic. Gang and Golan used a graphical approach to describe the stability of gas lift wells, the procedure originally presented by Gilbert (1954). By analyzing the inflow characteristics (IPR), lifting relationship (TPR), gas injection relationship (GPR), and discharge of gas (DPR) through the gas lift valve, they could determine the equilibrium points in the system. These points describe the conditions at which steady-state flow occur. Gang and Golan plotted (figure 4.4.1) the GPR and DPR as a function of gas injection rate, and picked the two intersection points as steady-state solutions of the system.

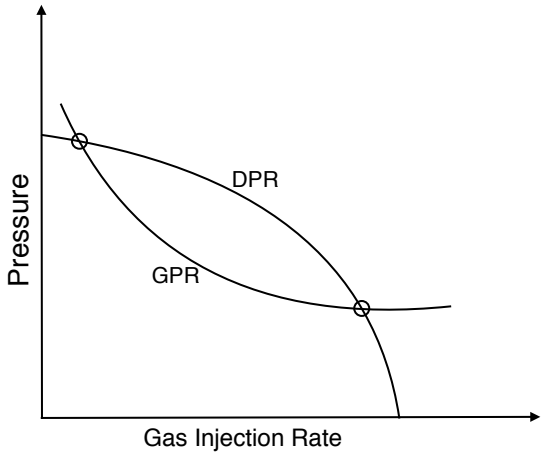

Figure 4.4.1: Equilibrium points and static stability.

Under the condition that the annulus pressure is constant, they claimed that the left point represents a stable solution while the right equilibrium point is subjected to static instability. At equilibrium point to the right, a temporary increase in the flow rate above the equilibrium rate requires less pressure to preserve the flow than the pressure available (from the reservoir). Thus, the flow rate is demanded to increase further and will not return to the original value. The opposite applies to the point to the left (Gang and Golan, 1989). Based on the analysis, Gang and Golan discovered that a small injection port size and choking at the wellhead are stabilizing.

The authors suggests that the static stability should be investigated by considering the required and available pressure-rate relationship in the production system, and proposed the following criterion for static stability.

$$\frac{dp_{available}}{dq_{flow}} < \frac{dp_{required}}{dq_{flow}}. \tag{4.4.1}$$

Gang and Golan focused their study on steady-state flow and static instability but emphasized that even if an equilibrium is statically stable, it may still be unstable due to systematic instabilities. They mentioned the interaction between the surface and downhole injection orifice and claimed that the sizes must be compatible if not severe oscillations could occur (Gang and Golan, 1989).

4.5 Alhanati et al.

Alhanati et al. (1993) investigated formerly proposed stability criteria in the literature and extended the criteria developed by Asheim (1988). They wanted to arrive at a more general stability criteria and extended Asheim‘s criteria by taking into account different flow regimes at the surface injection valve and the downhole injection valve. Like Gang and Golan (1989), Alhanati et al. analyzed the effect of inflow and outflow on stability in gas lift wells. They claimed steady-state procedures are inadequate and postulated; "Examining only inflow and outflow performance curves, as was done in the way suggested by Gang and Golan, is not sufficient for a proper continuous gas lift stability analysis; rather, a different approach than that used for flowing wells is necessary" (Alhanati et al., 1993).

Alhanati et al. compared the criteria developed by Asheim (1988) and Blick et al. (1988) and claimed that Asheim‘s criteria are easier to use as they only involve parameters employed in the design and operation of the well. The derivation of the new criteria, however, was inspired by the mathematical model of Blick et al., but the results are still closer to Asheim‘s. Like Asheim, they neglect frictional forces in the production tubing which they agree will make the criteria more conservative since friction has a dampening effect on the system (Alhanati et al., 1993).

Using the criteria, Alhanati et al. show that casing heading will not occur if the flow through the downhole injection valve is critical. This is inherent in the criteria developed by Asheim. If the injection rate does not change by a reduction in the well pressure, the fluid density in the well will increase as a result of increased inflow of reservoir fluid. This satisfies stability criterion F1 (equation 4.2.1). The authors recommend ways of stabilizing the well, and these include decreasing the volume of the annulus, reducing the size of the injection port, and increasing the flow rate of lift-gas. Alhanati et al. compared the criteria against field data and concluded the criteria gave qualitative indications on ways to avoid instabilities in gas lift wells (Alhanati et al., 1993).

4.6 Poblano et al.

Poblano et al. (2002) developed diagrams to facilitate the application of stability criteria. The diagrams, called stability maps, demonstrate regions of stable and unstable flow in gas lift wells, in addition to the operational limits of the system. By a numerical model of a gas lift well, field data, and existing stability criteria, stability maps were constructed to determine the stability of the well under certain conditions. A stability map, based on the criteria by Alhanati et al., is shown in figure 4.6.1. The map shows stability given as a function of the gas injection rate and the size of the downhole injection port. Any change to other well parameters will generate a new map, with a different stability limit associated with the operation (Poblano et al., 2002).

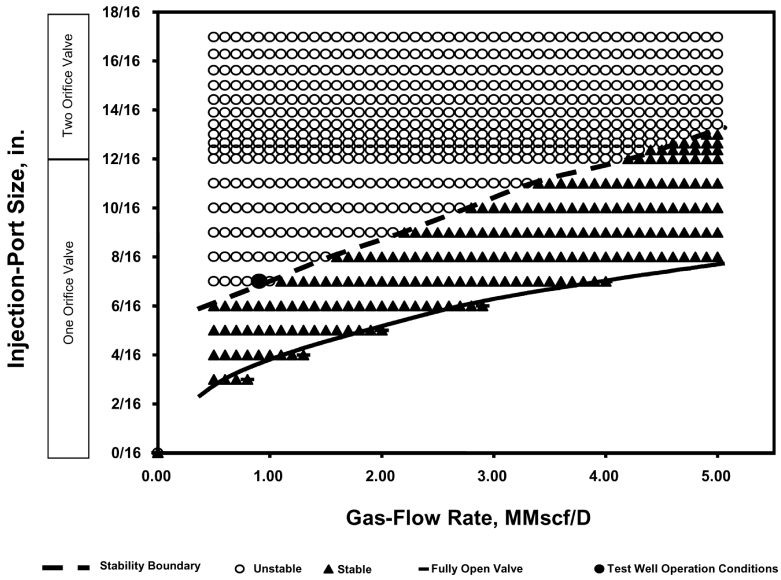

Figure 4.6.1: Stability map, injection ports size and gas injection flow rate (Poblano et al., 2002).

According to Poblano et al., the benefit of stability maps is a rapid and efficient assessment of the operation, and it can be used in the design of the gas lift system. The stability maps confirm that a small injection port size and high injection rate of lift gas stimulates stability. Also, the maps show a reduction in diameter of the production tubing has a stabilizing effect. The study showed the stability criteria by Asheim and Alhanati et al. correlate well with the actual conditions in the test well. Poblano et al. declared stability maps as a useful tool in well planning and design.

4.7 Fairuzov et al.

Fairuzov et al. (2004) modified the stability maps developed by Poblano et al. and used the wellhead pressure as the ordinate axis in the new maps. They believed this modification was more appropriate since the wellhead pressure and injection rate are parameters that easily can

be measured and controlled during production. New stability criteria were developed, and data from a deep offshore gas lift well in the Akal field were used for comparison with existing criteria. Figure 4.7.1 show the stability boundaries predicted by the different criteria. It is worth noting that the new stability map also shows the conditions in which the well cannot operate due to low gas rate in combination with high wellhead pressure.

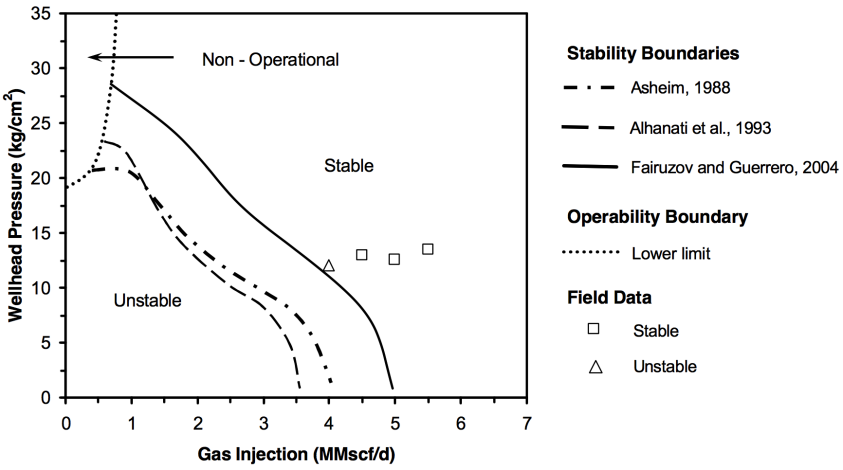

Figure 4.7.1: Stability map, wellhead pressure and gas injection flow rate (Fairuzov et al., 2004).

Fairuzov et al. discovered that existing stability criteria underestimated the unstable region and claimed the new criteria provides a more accurate prediction of the stability threshold. Among their findings, they observed that increased productivity index was strongly stabilizing, which confirms the observations made by Asheim. Fairuzov et al. believed that this information could be used to identify well damage and the effect of stimulation. They also pointed out that instability can be caused by a drop of the pressure in the gas supply network, e.g., in the event of a temporary shutdown of compressors or other disturbances (Fairuzov et al., 2004).

4.8 Comparison of theories

The main features of the above stability theories are in general the same, and they all say gas lift instability is a phenomenon that entails production problems. The theories indicate that proper well design may help ensure stable production throughout the well's life. The stability theories also agree on the stabilization measures that may be implemented in the system. Among others, the most suggested measures are increased gas injection rate, decreased injection orifice size, and reduced annular volume. Decreasing the annular volume, however, may usually be accomplished only in the design phase.

Thus, thorough analyses should be performed in the design stage to identify potential stability problems before the well is completed. In this way, unnecessary interventions and production shutdowns are avoided.

The stability criteria derived by Asheim (1988) are often the easiest to use in practice and form the basis for several of the more recent and more complex theories. Common to all criteria is that they are based on several simplifying simplifications and assumptions, and the extension by Alhanti et al. (1993) include many of the same assumptions as the criteria by Asheim.

Poblano et al. (2002) used the criteria of Asheim and Alhanati et al. as limit values in their stability criteria, and discovered the criteria correlated well with the conditions in the test well. Fairuzov et al. (2004), on the other hand, claimed the criteria underestimated the unstable region in the map. With attention to Asheim's criteria, they are both based solely on the downhole response and does not take into account the conditions at the outlet of the production tubing. This may affect their prediction power.

In more recent times in his doctoral thesis, Hu (2004) claimed that existing stability criteria are difficult to use today because wells have become far more complicated than before. Especially regarding completion and flow. The conditions will vary from well to well, and often other factors need to be taken into account when choosing the stabilization method. Also, the prediction of future well conditions is often very challenging, and this too makes it harder to select the best way of stabilization. Therefore, the consequence of unstable gas lift wells may give considerable uncertainties in the production forecast and operational costs (Hu, 2004).

Chapter 5

Active feedback control and stability

During the 1990s, reports suggested cybernetic approaches to eliminate flow instability in gas lift wells. Studies showed that equipping wells with an automatic feedback control system could both reduce instability and increase production. Automatic feedback control implies that settings of one or more adjustable elements in the well, i.e. choke or orifice opening, are automatically decided based on one or more measurements in the same system (Dalsmo and Halvorsen, 2002).

5.1 Dalsmo and Halvorsen

Dalsmo and Halvorsen (2002) employed an active feedback control solution on a gas lift well in the Brage field. To control the production, downhole pressure measurements in the well were used to estimate the opening of the production choke at the wellhead. In an attempt to control the test well manually, pressure and flow rates showed severe oscillations, and after a short production period, the well had to be shut-in.

When the control system was activated the pressure and flow variations were eliminated, and the flow stabilized (Dalsmo and Halvorsen, 2002). Dalsmo et al. concluded that the benefit of employing automatic feedback control in unstable gas lift wells was evident, and decided to launch another test program utilizing similar control system.

5.2 Hu and Golan

Hu and Golan (2003) investigated the benefit of active feedback control on production loss in unstable gas lift wells. Using a dynamical simulator, the bottomhole flowing pressure was controlled by the production choke to simulate the effects of feedback control on production.

By simulation Hu and Golan demonstrates that both casing heading and tubing heading instability may be stabilized by the active feedback controller. For casing heading, the simulation shows that 17 % of production can be saved using feedback control on the well. In the case of tubing heading instability, 20 % of production is saved. Hu and Golan concludes that active feedback control gives a new option to both stabilize the well and optimize production (Hu and Golan, 2003).

5.3 Eikrem et al.

Eikrem et al. (2008) proposed three simple control structure to stabilize gas lift instability in simulations and laboratory experiments. The authors investigated the use of downhole, casing-head, and differential pressure as the set point for the controller to stabilize flow instability.

Both the simulations and the laboratory experiments gave promising results and all control structures successfully stabilized production. Eikrem et al. claimed the findings shows that it is possible to use different control structures to eliminate instability. In the event sensor failure or other issues, it is possible to switch from one control structure to another (Eikrem et al., 2008).

Chapter 6

Dynamic gas lift model

Regarding existing stability criteria, experience seems to show that when they predict instability, the gas lift well will most likely be unstable. When the criteria predict stability, however, the well may turn out to be unstable in practice (Alhanati et al., 1993).

The existing stability criteria do not take into account the flow at the outlet of the production pipe, and this has been a motivation for the work undertaken in the thesis. The model to be tested considers the outflow variations explicitly, and it is reasonable to believe that this will improve the prediction power.

6.1 General model

Hjalmars (1973) investigated the flow instability in airlift pumps by perturbation analysis. Fitremann and Vedrines (1985) developed a numerical model of a gas lift well in similar manner, and Asheim (1988) developed simple stability criteria for gas lift by considering how the system respond to small perturbations. Since then, extensions and improvements have been suggested to predict stability in gas lift wells (Fairuzov et al., 2004; Poblano et al., 2002; Alhanati et al., 1993).

The existing criteria considers change due to current state and may be expressed as

$$\frac{d}{dt}X\left(t\right) = AX\left(t\right). \tag{6.1.1}$$

Where X is a vector of state variables such as pressures or rates and t is the current time. A is a matrix of coefficients relating the well design and reservoir parameters.

With active feedback control, control variables such as valve opening can continuously be adjusted based on measurements. This constitute to an additional term in the model.

$$\frac{d}{dt}X\left(t\right) = AX\left(t\right) + BU\left(t\right). \tag{6.1.2}$$

Where U is a vector containing the control variables and B is a matrix specifying how the control variables affect the system.

6.2 Current model

Figure 6.2.1 represents the gas lift system considered. Gas is pumped down into the annulus at a constant rate, and the produced fluids flow into a pressure-controlled separator. Thus, the tubing head pressure may be considered constant. The lift-gas enters the tubing through a downhole injection valve and mixes with the fluids from the reservoir. This reduces the density of the fluid mixture and thereby lowers the pressure at the bottom of the well such that the inflow from the reservoir increases.

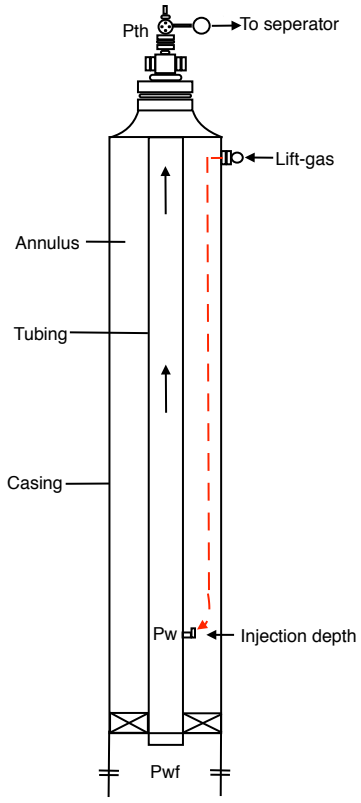

Figure 6.2.1: Simplified gas lift model.

6.2.1 Steady-state gas lift

The relations used apply to stationary/steady flow at given input pressure, temperature, and flow rate. A steady-state flow model has been constructed, and along the production pipe, it is assumed the mass flow is constant, while pressure and temperature change. The model enables calculation of pressure changes along the production pipe, and thus also phase relationship, volume rate, and velocity. The model accounts for slip between gas and liquid while liquid holdup has been neglected. To match the model output with the provided well data, the slip parameters are tuned. Although the model output matches the measured data, this does not necessarily mean the flow modeling is correct. However, it provides a basis for estimating the conditions down in the well.

A slightly different steady-state gas lift model has also been constructed. The model estimates pressure and flow rates in the same manner as the model described above. However, for certain downhole pressure, wellhead pressure, gas-oil ratio, and water cut the model estimates the required oil rate for a given injection rate.

The mixture of injected gas and reservoir fluid flows up along the production tubing. At steady-state flow, the pressure gradient in the well is estimated as in equation 6.2.1.

$$\frac{dp}{dx} + \rho_{TP} g_x + \frac{1}{2} f_{TP} \frac{\rho_{TP}}{d} v_m^2 = 0. \tag{6.2.1}$$

The bottomhole pressure may be expressed by integrating equation 6.2.1 along the production tubing.

$$p_w = p_{th} + \bar{\rho_{TP}} g_x + \frac{1}{2} \bar{f_{TP}} \frac{\bar{\rho_{TP}}}{d} \bar{v_m}^2 L. \tag{6.2.2}$$

The inflow of reservoir fluid is expressed by the steady-state pressure drop between the reservoir and the bottom of the well.

$$p_w = p_r - \frac{Q_l}{J_w}. \tag{6.2.3}$$

Where J_w is the productivity index, indicating downhole rate. Lift-gas is injected at the wellhead and flows down the annulus. Assuming the flow velocity is low, the pressure at the injection depth x can be approximated by the barometric equation.

$$p_g(x) = p_{wh} \exp \frac{M_g x}{zRT}. \tag{6.2.4}$$

At the depth of the injection point the lift-gas flows into the production tubing through an orifice valve. For a constant valve opening, the pressure drop across the valve may be expressed by the orifice equation.

$$\Delta p_c = p_g - p_w = \frac{1}{2}\frac{\rho_g}{A_c^2}Q_g^2. \tag{6.2.5}$$

6.2.2 Dynamic response

The dynamic response is estimated by considering how the gas lift system at steady-state is affected by small disturbances. The current model is developed and provided by Asheim (2017). The model includes outflow variations and results in a time delay. The model structure may be expressed as

$$\frac{d}{dt}X\left(t\right) = AX\left(t\right) + DX\left(t - \Delta t\right). \tag{6.2.6}$$

Where D is the delay-matrix depending on well design and reservoir parameters. A, t, and x are defined as in equation 6.1.1.

Production tubing

The steady-state pressure drop along the tubing may be expressed by equation 6.2.2. Differentiating equation 6.2.2 and perturbating gives the tubing pressure response due to change in density of the fluid mixture.

$$\frac{\vartheta}{\vartheta t}\delta p_w = \frac{\vartheta}{\vartheta t}\delta p_{tp} + \left(g_x + \frac{1}{2}f_m\frac{v_m^2}{d}\right)L\frac{\vartheta}{\vartheta t}\delta\bar{\rho_{TP}} + f_m\frac{\bar{\rho_{TP}}}{d}v_m L\frac{\vartheta}{\vartheta t}\delta v_m + \frac{1}{2}f_m\frac{\bar{\rho_{TP}}}{d}L\frac{\vartheta}{\vartheta t}\delta v_m^2. \tag{6.2.7}$$

Density change will occur if the relationship between the flowing gas and liquid changes. This can be quantified using the continuity equation, $\vartheta/\vartheta t\rho_{TP} + \vartheta/\vartheta x(\rho_m v_m)$. Integrating from inlet to outlet, along the tubing, this gives

$$\frac{\vartheta}{\vartheta t}\delta\bar{\rho_{TP}} = \frac{1}{L}\left[\left(\rho_g v_{sg} + \rho_l v_{sl}\right)_{x=0} - \left(\rho_g v_{sg} + \rho_l v_{sl}\right)_{x=L}\right]. \tag{6.2.8}$$

The outflow, at $x = L$, is a mixture that can be quantified by the product of the density, $\rho_m = (\rho_g v_{sg} + \rho_l v_{sl})/v_m$, and the mixture velocity, $v_m = v_{sg} + v_{sl}$. Neglecting slip, the mixture in tubing has the velocity v_m and will therefore reach the outlet after time, $\Delta t = L/v_m$. The relation in equation 6.2.8 may be expressed as

$$\frac{\vartheta}{\vartheta t}\delta\bar{\rho_{TP}} = \frac{1}{L}\left[\left(\rho_g v_{sg} + \rho_l v_{sl}\right)_t - \left(\rho_m v_m\right)_{t-\Delta t}\right]. \tag{6.2.9}$$

If the inflow changes the density and velocity of the fluid mixture will change. The velocity change will propagate as pressure waves and will quickly affect the flow at the outlet. Changed inflow gas-oil ratio and mixture density will follow the stream, thus propagate much slower. Assuming changes in velocity are noticed immediately at the outlet, perturbation of equation 6.2.9 gives

$$\frac{\vartheta}{\vartheta t}\delta\bar{\rho_{TP}} = \frac{1}{L}\left[\left(\rho_g \delta v_{sg} + \rho_l \delta v_{sl}\right)_t - \left(\rho_m v_m\right)_t - \left(\rho_m v_m\right)_{t-\Delta t}\right]. \tag{6.2.10}$$

According to the definitions of mixture density and velocity, perturbation gives

$$\Delta\rho_m = \frac{\left(v_m \delta\left(\rho_g v_{sg} + \rho_l v_{sl}\right) - \left(\rho_g v_{sg} + \rho_l v_{sl}\right)\delta v_m\right)}{v_m^2}, \tag{6.2.11}$$

and

$$\delta v_m = \delta v_{sg} + \delta v_{sl}. \tag{6.2.12}$$

Substituting the above results into equation 6.2.7 relates the change of well pressure to the inflow variation. To express in terms of volume rates, the superficial velocities are multiplied by the tubing cross sectional area. Using the definition of flux fraction, $\lambda_i = Q_i/(Q_g + Q_l)$, this gives

$$\frac{\vartheta}{\vartheta t}\delta p_w = f_m \frac{\bar{\rho_{TP}}}{d} v_m L \frac{\vartheta}{\vartheta t}\delta v_m + \frac{\Delta\rho g_x L}{V_t}\left[\left(\lambda_g \delta Q_l - \lambda_l \delta Q_g\right)_t - \left(\lambda_g \delta Q_l - \lambda_l \delta Q_g\right)_{t-\Delta t}\right]. \tag{6.2.13}$$

$$\frac{\vartheta}{\vartheta t}\delta p_w = f_m \frac{\bar{\rho_{TP}}}{A_t d} v_m L \left(\frac{\vartheta}{\vartheta t}\delta Q_g + \frac{\vartheta}{\vartheta t}\delta Q_l\right) + \frac{\Delta\rho g_x L}{V_t}\left[\left(\lambda_g \delta Q_l - \lambda_l \delta Q_g\right)_t - \left(\lambda_g \delta Q_l - \lambda_l \delta Q_g\right)_{t-\Delta t}\right]. \tag{6.2.14}$$

Annulus

Pressure change in the annulus will propagate with sonic speed. This gives such a rapid response that the pressure can be considered in stationary equilibrium and expressed by the equation of state $p_g V_a = znRT$. At the wellhead, constant lift-gas rate is assumed to enter the annulus. At steady-state conditions, equal rate of lift-gas flows out through the injection valve, thus mass conservation. If the rate through the injection rate deviates, the amount of gas in the annulus will change.

According to the equation of state, the pressure response becomes

$$\frac{\vartheta}{\vartheta t}\delta p_g = -\frac{p_g}{V_a}\delta Q_g. \tag{6.2.15}$$

Where δQ_g express the deviation from steady-state injection rate at downhole temperature and gas pressure, p_g.

Inflow

Fluid flow from the reservoir may be expressed as in equation 6.2.3. Within shorter periods of time , the reservoir pressure and productivity index may be considered constant. Perturbating then gives the dynamic response

$$\delta Q_l = -B_o J \delta p_w = J_w \delta p_w. \tag{6.2.16}$$

The inflow of gas usually takes place through a nozzle at the injection valve. Perturbation of equation 6.2.5 show that the pressure deviations, δp_g and δp_w, affect gas inflow as follows

$$\delta Q_g = J_g \delta p_g - J_g \delta p_w. \tag{6.2.17}$$

Where,

$$J_g = \frac{A_c^2}{\rho_g Q_g}. \tag{6.2.18}$$

Here, A_c is the orifice opening and J_g the "gas inflow index".

System response

The dynamic response of the gas lift system results from interaction between tubing and annulus. By substituting equation 6.2.17 into equation 6.2.15 provides the annular pressure response in terms of pressure deviation.

$$\frac{\vartheta}{\vartheta t}\delta p_g = -\frac{p_g}{V_a}\left(J_g \delta p_g - J_g \delta p_w\right)_t. \tag{6.2.19}$$

By substituting equation 6.2.16 and 6.2.17 into 6.2.14 provides the tubing response.

$$\begin{aligned}\frac{\vartheta}{\vartheta t}\delta p_w = &\left[a_w \delta p_w - a_g \delta p_g - f_m \frac{\bar{\rho_{TP}}}{d} v_m \frac{L}{A_t}\left(J_g + J_w\right)\frac{\vartheta}{\vartheta t}\delta p_w + f_m \frac{\bar{\rho_{TP}}}{d} v_m \frac{L}{A_t} J_g \frac{\vartheta}{\vartheta t}\delta p_g\right]_t \\ &- \left[a_w \delta p_w - a_g \delta p_g\right]_{t-\Delta t}.\end{aligned} \tag{6.2.20}$$

By combining equation 6.2.15 and 6.2.17 the tubing response may be further expressed as

$$\frac{\vartheta}{\vartheta t}\delta p_w = \left[a_w\delta p_w - a_g\delta p_g - f_m\frac{\bar{\rho_{TP}}}{d}v_m\frac{L}{A_t}\left(J_g + J_w\right)\frac{\vartheta}{\vartheta t}\delta p_w + f_m\frac{\bar{\rho_{TP}}}{d}v_m\frac{L}{A_t}J_g\left(c\delta p_w - c\delta p_g\right)\right]_t - \left[a_w\delta p_w - a_g\delta p_g\right]_{t-\Delta t}. \tag{6.2.21}$$

By expressing the parameter groups in terms of response coefficients, equation 6.2.19 and 6.2.21 becomes

$$\frac{\vartheta}{\vartheta t}\delta p_g = -\frac{p_g}{V_a}\left(J_g\delta p_g - J_g\delta p_w\right)_t = \left(c\delta p_w - c\delta p_g\right)_t, \tag{6.2.22}$$

and

$$\left(1 + f_tJ_g + f_tJ_w\right)\frac{\vartheta}{\vartheta t}\delta p_w = \left(a_w + cf_tJ_g\right)_t\delta p_w - \left(a_g + cf_tJ_g\right)_t\delta p_g - \left(a_w\delta p_w - a_g\delta p_g\right)_{t-\Delta t}. \tag{6.2.23}$$

The response of the gas lift system may described by the two equations above. With linearization around a steady-state solution of the system, the coefficients become constants. On matrix form, the two equations form a delay-differential equation given as

$$\epsilon^{-1}\frac{\vartheta}{\vartheta t}\begin{bmatrix}\delta p_w\\ \delta p_g\end{bmatrix} = \begin{bmatrix}a_w + cf_tJ_g & -\left(a_g + cf_tJ_g\right)\\ c & -c\end{bmatrix}\begin{bmatrix}p_w\\ p_g\end{bmatrix}_t - \begin{bmatrix}a_w & -a_g\\ 0 & 0\end{bmatrix}\begin{bmatrix}p_w\\ p_g\end{bmatrix}_{t-\Delta t} \tag{6.2.24}$$

Where ϵ = $\left(1 + f_tJ_g + f_tJ_w\right)$. Setting $a_1 = \epsilon\left(a_w + cf_tJ_g\right)$, $b_1 = \epsilon\left(a_w + cf_tJ_g\right)$, $a_2 = \epsilon a_w$, and $b_2 = \epsilon a_g$ the differential equation may be expressed as

$$\frac{\vartheta}{\vartheta t}\begin{bmatrix}\delta p_w\\ \delta p_g\end{bmatrix} = \begin{bmatrix}a_1 & -b_1\\ c & -c\end{bmatrix}\begin{bmatrix}p_w\\ p_g\end{bmatrix}_t - \begin{bmatrix}a_2 & -b_2\\ 0 & 0\end{bmatrix}\begin{bmatrix}p_w\\ p_g\end{bmatrix}_{t-\Delta t} \tag{6.2.25}$$

The first part of equation 6.2.25 refers to the current time t and considers the variations downhole at the injection depth. The second part, $t - \Delta t$, accounts for the kinematic delay between the inflow and outflow. Mixture variations generated downhole will propagate along the tubing and exit at a later time. The changes are accounted for by the delay term.

The system parameters ϵ, a_w, a_g, c, f_t, J_g, and J_w relate functionally to reservoir, fluid properties and well design. Given fluid and reservoir properties and gas lift design, the response parameters and matrix coefficients may be estimated. The dynamic response of the gas lift system may then be estimated from equation 6.2.25.

6.3 Comparison with existing criteria

The derivation of the current model is based on the perturbation method by Asheim (1988), but contain some differences and improvements. Most important, the model includes the delayed response that represents outflow density variations. Also, the suggested model accounts for flow friction along the production tubing. The annular response, however, is the same to what Asheim (1988) considered in his criteria. If the delayed response is neglected, equation 6.2.24 simplifies as

$$\frac{\vartheta}{\vartheta t}\begin{bmatrix}\delta p_w \\ \delta p_g\end{bmatrix} = \begin{bmatrix}\epsilon\left(a_w + cf_tJ_g\right) & -\epsilon\left(a_g + cf_tJ_g\right) \\ c & -c\end{bmatrix}\begin{bmatrix}p_w \\ p_g\end{bmatrix}_t \tag{6.3.1}$$

Neglecting flow friction gives f_t = 0 and leads to, ϵ = 1, $a_1 = a_w$, and $b_1 = a_g$. Equation 6.3.1 may than be written as

$$\frac{\vartheta}{\vartheta t}\begin{bmatrix}\delta p_w \\ \delta p_g\end{bmatrix} = \begin{bmatrix}a_w & -a_g \\ c & -c\end{bmatrix}\begin{bmatrix}p_w \\ p_g\end{bmatrix}_t \tag{6.3.2}$$

The expression above represents a homogeneous linear equation, and the stability of such systems is completely determined by its eigenvalues (Hirch and Smale, 1974). The eigenvalues may be expressed as

$$\lambda = \frac{1}{2}\left[(a_w - c) \pm \sqrt{(a_w - c)^2 - 4c(a_g - a_w)}\right]. \tag{6.3.3}$$

The eigenvalues may be real or complex of the form $\lambda = \alpha + i\omega$. In many cases the eigenvalues are complex, and stability of the system requires all eigenvalues to have negative real part, $\alpha = a_w - c < 0$. Negative real part implies damped oscillations and thus stable system. Inserting the expressions for a_w and c into the inequality gives (Asheim, 2016)

$$\frac{1}{V_t}\frac{\Delta\rho g_x L}{Q_g + Q_l}\left(\frac{A_c^2 Q_l}{\rho_g Q_g} - J_w Q_g\right) > \frac{1}{V_a}\frac{p_g A_c^2}{\rho_g Q_g}. \tag{6.3.4}$$

The above equation imitates the depletion response, equation 4.2.2, proposed by Asheim (1988) and shows the model reduces to existing criteria under certain considerations. The inequality illustrates how important well and reservoir parameters affect stability in gas lift wells. The purpose of the comparison is simply to show that the current model is an extension of existing stability criteria and that some modifications have been made to improve its prediction power hopefully. In the following chapters, however, the delay-differential equation 6.2.25 form the basis for the gas lift stability analysis.

Chapter 7

Gas lift stability study

The analysis in the subsequent chapters investigate the stability of a gas lift well and is intended to check the suggested model. The theoretical model is a simplification, and the dynamic response predicted by the model needs to be checked against measured data.

The characteristics of different production modes will be discussed, and estimates of static and dynamic parameters are presented. The initiation of flow instability is examined in detail, and the wells ability to oppose variations of particular characteristics are explored. The findings provide the basis for further analysis, and in Chapter 8 the theoretical model is applied to the production data.

7.1 The Heidrun case

The provided data consists of measurements from well 6507/7-A-23 in the Åre formation, located in the Heidrun field in the Norwegian Sea. The Åre formation consists of lower and middle Jurassic sandstone, and the reservoir is heavily faulted. The primary recovery strategy in the formation is water injection The well is operated by Statoil and has been producing oil since late 2000. Due to declining reservoir pressure and reduced deliverability, the well was put on gas lift in 2010 to improve production (Norwegian Petroleum Directorate, 2017). Since early 2016, the well has occasionally been subjected to flow instabilities.

7.1.1 Data availability

The provided well data were measured throughout the year 2016 and January-February 2017, and consist of measurements taken once every minute. The data include measurements of temperatures, pressures, surface flow rates, and choke settings. Temperature and pressure data are available at the wellhead and downhole conditions. The pressure in the annulus and the gas lift supply pressure, are also provided. The flow rate measurements were acquired using a multiphase flow meter and include lift-gas, gas, oil, and water rates at surface conditions.

The accuracy of the multiphase meter is unknown. However, the author is aware of the issue and that there might be inconsistencies between measured and actual rates.

Data on the particular reservoir are scarce in the literature. However, the necessary fluid properties have been provided by Statoil. The lift-gas has been assumed to have the same properties as the produced reservoir gas.

7.1.2 Well design and completion

The well is deviated, and the total measured depth (MD) is 3022 meters. The true vertical depth (TVD) is 2485 meters. The well is perforated at approximately 2900 meters MD. The downhole temperature and pressure gauge are set at 2670 meters MD. The well is equipped with a 1.5" orifice injection valve with a 23/64" nozzle installed at 1826 meters MD. The well is completed with a 5.5" tubing and a 9 5/8" production casing. Figure 7.1.1 shows a simplified model of the well. The figure is neither in the correct scale nor deviated and is only intended to illustrate the main components of the gas lift system. The schematic also shows the position at the wellhead and downhole at which the pressure and temperature measurements were acquired, indicated with PT/TT.

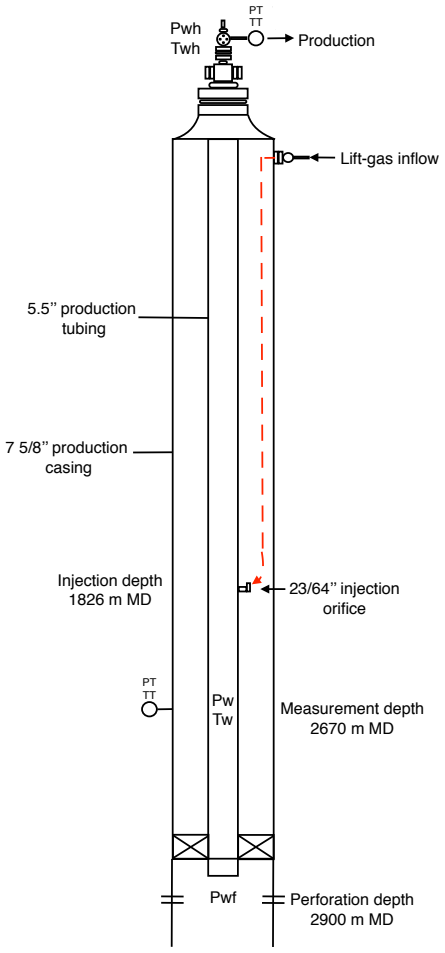

Figure 7.1.1: Well 6507/7-A-23 schematic.

7.2 Production measured

The provided data have been split into sub-periods, on a two-month basis, to give a better overview of the production characteristics. The stability analysis focuses on three out of the in total seven sub-periods of measurements. The selected periods consist of March-April 2016, May-June 2016, and January-February 2017. These data sets have been selected for further analysis because they contain different production characteristics and thus provide a basis for examining the well under various conditions.

The figures that follow show measured liquid (oil and water) rates. The purpose is to give the reader a quick overview of what is available and may be expected in the well. The red and blue dotted lines illustrate the standard deviation and the mean of production respectively.

Figure 7.2.1-7.2.3 below and on the next page show periods of varying production rates. Alternating periods of stationary production appear to develop sudden oscillations. Often, the oscillations are only temporary, and production returns to normal after a couple of hours. At other times, however, the system develop oscillations that are more persistent and last for several days to weeks.

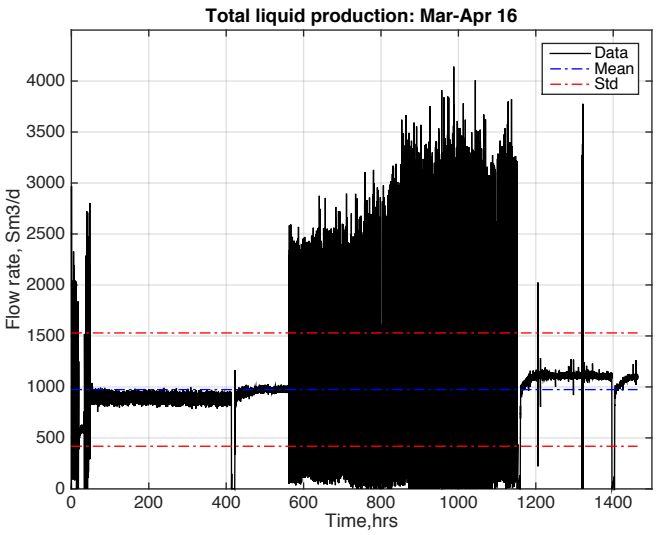

Figure 7.2.1: Liquid production March - April 2016.

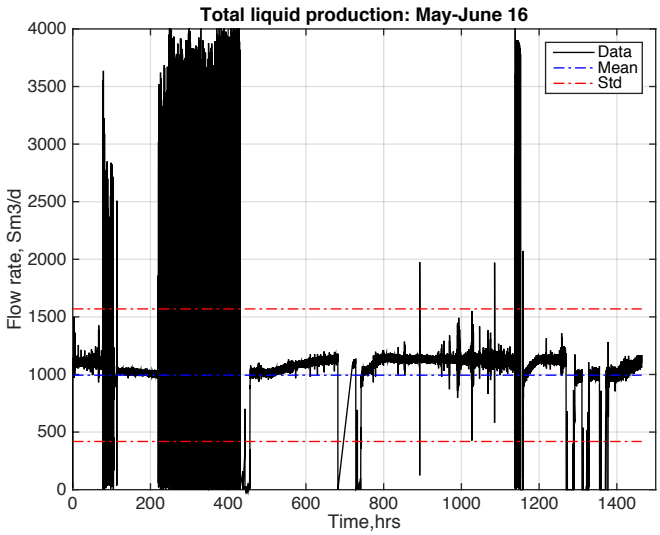

Figure 7.2.2: Liquid production May - June 2016.

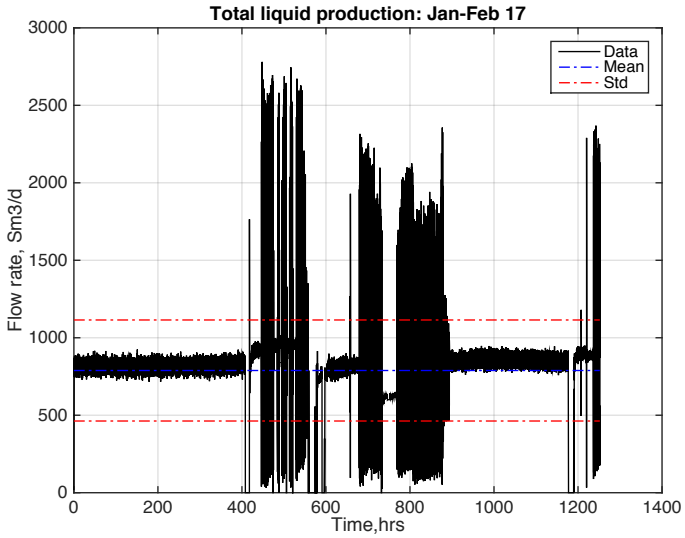

Figure 7.2.3: Liquid production January - February 2017.

An interesting observation is that significant oscillations occur almost suddenly and without any gradual buildup. The measurements also consist of intervals of what seems to be stationary production, of relatively long duration. The different intervals facilitate for comparison between various production modes and may enable us to understand under what conditions the system becomes unstable. Thus, it could be of interest to examine intervals of production shortly before oscillations develop in the system.

At times the data show intervals in which the well is shut-in after periods of severe oscillations. The production stop may be due to operational problems in the processing facilities and other surface equipment, or an attempt to gain control over the well.

7.3 Characterization and parameter estimation

To characterize the production in the well, data in the interval January-February 2017 have been selected for a more in-depth study. Figure 7.3.1 illustrates the liquid production for the period. The period seems to include ranges of different production modes, and this makes it possible to study the behavior of the system under different circumstances. The various conditions also allow for estimation of system parameters and may provide a significantly better insight than analysis based on only a single production mode. The period January-February 2017 seems to be comprised of ranges of stationary production, static pressure build-up/shut-in, and oscillating production.

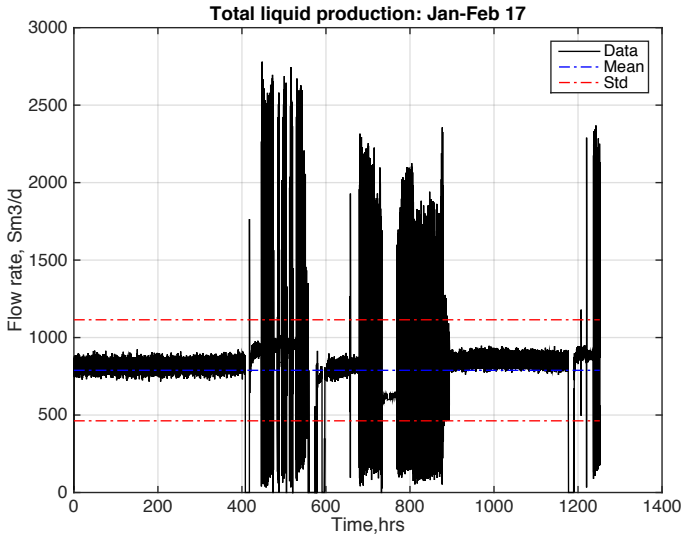

Figure 7.3.1: Liquid production January - February 2017.

The production measurements January-February 2017 seems to include the following production modes:

- Stationary production: 0 - 400 hours.
- Oscillating production: 680 - 710 and 785 - 805 hours.
- Static pressure build-up: 1177 - 1190 hours.

7.3.1 Stationary production

Figure 7.3.2 shows the liquid rate variation during the first three days of January 2017. An interval of 72 hours has been selected to visualize the variations around the mean of the production better. The mean and the standard deviation of the liquid rate in the interval t = 0-400 hours is estimated to be 819.4 Sm^3/d and 26.9 Sm^3/d respectively.

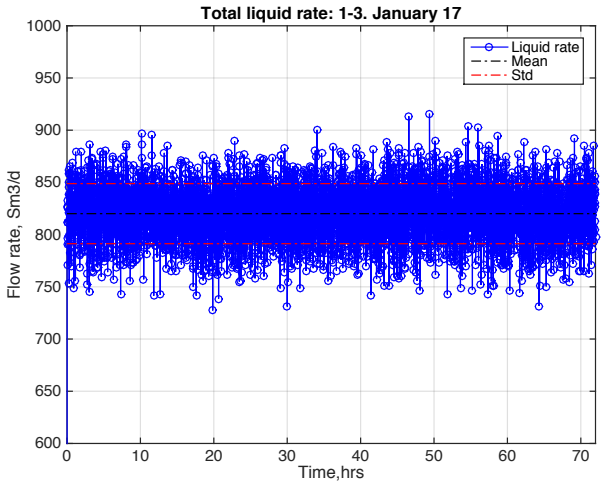

Figure 7.3.2: Liquid production rate 1-3. January 2017.

To check for stationarity, figure 7.3.3 shows the probability density function (pdf) of the flow rate data in the assumed stationary production interval. The measurements exhibit the characteristic bell shape of normally distributed data. The red line is a theoretical pdf fitted to the data with same mean and standard deviation. The good fit indicates the measurements are close to perfect normal distributed and that the data vary stochastic around the mean.

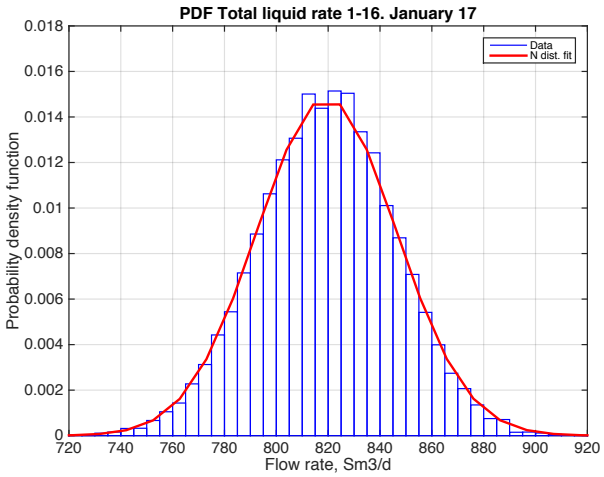

Figure 7.3.3: Probability density function liquid production rate 1-16. January 2017.

Analysis of the frequency spectrum does not reveal any stable oscillation present in the data. Based on the discovery above, the production may be considered stationary during the first 17 days of January 2017. It is worth noting the average fluids production in the interval t = 0-400 hours was 819.4 Sm^3/d and the average in the interval t = 0-72 hours was 820.0 Sm^3/d. The closeness supports the assumption of stationary production in the first 400 hours of January 2017.

Stationary reference

The stationary production period provides a basis for estimating parameters in the well using the steady-state gas lift model. The stationary reference is built on averages of the production data in the interval t = 0-400 hours. Table 7.3.1 summarizes the input parameters for the steady-state model.

Table 7.3.1: Input steady-state model 1-16. January 2017

Parameter	
Wellhead pressure, [bar]	22.3
Downhole pressure, [bar]	122.5
Oil rate, [Sm^3/d]	263.3
Water rate, [Sm^3/d]	556.1
Gas rate, [Sm^3/d]	1.38 10^5
Injection rate, [Sm^3/d]	8.85 10^4
Gas injection pressure wellhead, [bar]	118.9
Injection orifice diameter, [mm]	9.1

Figure 7.3.4 on the next page shows estimated pressure profiles in tubing and annulus for the rate and pressure conditions in the table above. Adjusting the slip parameters gives a pressure of 122.5 bars at the downhole measuring point. This is the same as the average of the measured well pressure. Injection of lift-gas at a depth of the injection valve (1826 meters MD) will reduce the pressure gradient up the production tubing, and this may be observed from the change in the blue pressure curve.

The tubing pressure at the injection depth is estimated to 68.6 bars, and the pressure at the bottom of the well is estimated to 138.2 bars. The figure also shows pressure in the annulus for injection pressure at the wellhead as given above. It is assumed gas-filled annulus down to the injection valve and liquid-filled below. At the injection depth, this provides a pressure difference annulus-tubing of 64.6 bars.

According to the orifice formula, equation 6.2.5, injection of lift-gas through the given orifice size should cause a pressure drop of 7.6 bars. The inconsistency of the two pressure differences is obvious and may be due to errors in estimating the pressure gradient in the annulus or an error in the provided data. In the model calculations later in the report, however, the pressure drop given by the orifice equation has been assumed correct and will be used as a reference for the pressure in the annulus.

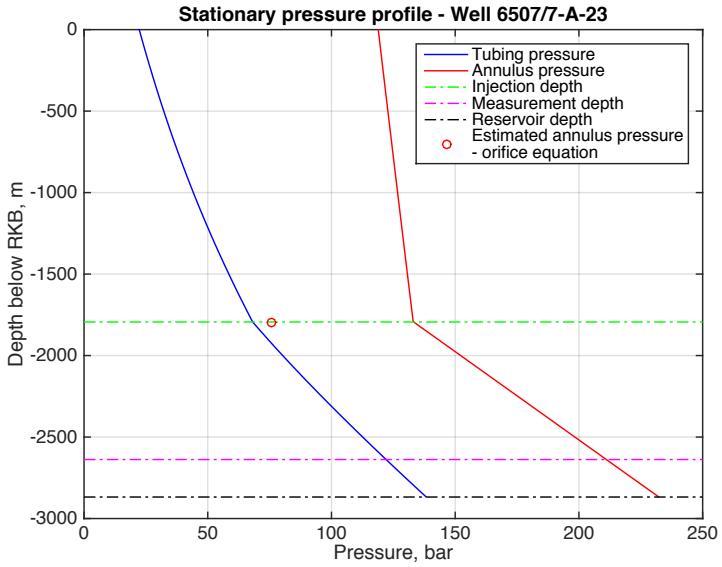

Figure 7.3.4: Stationary pressure profile for production tubing and annulus.

Stationary productivity index

Based on stationary production, interval t = 0-400 hours, the stationary productivity index in the well may be estimated. During stationary production, the gas lift model estimates the pressure at the bottom of the well to be 138.2 bars. Average liquid production was 819.4 Sm^3/d.

From the pressure build-up period (section 7.3.2), the reservoir pressure has been approximated to around 171 bars. When the measurements were acquired the stationary production and static pressure buildup was close in time. Thus the reservoir pressure was likely to be similar. Utilizing the steady-state inflow relationship gives the resulting stationary productivity index

$$J = \frac{q_l}{p_r - p_w} = \frac{819.4 \frac{Sm^3}{d}}{(171.0 - 138.2) bar} = 25.06 \frac{\frac{Sm^3}{d}}{bar}. \tag{7.3.1}$$

Analysis of other periods of steady production gives similar values of the productivity index. Considering the uncertainty in the flowing bottomhole and reservoir pressure estimates it may be assumed that 25 $Sm^3/d/bar$ is a good representation of the well deliverability.

7.3.2 Static pressure build-up

Figure 7.3.5 shows measured well pressure 14-19. February 2017, interval t = 1100-1200 hours. The measurements show the well was shut in for 13 hours 18. February. The static pressure build-up provides a basis for estimating the reservoir pressure in the surrounding formation.

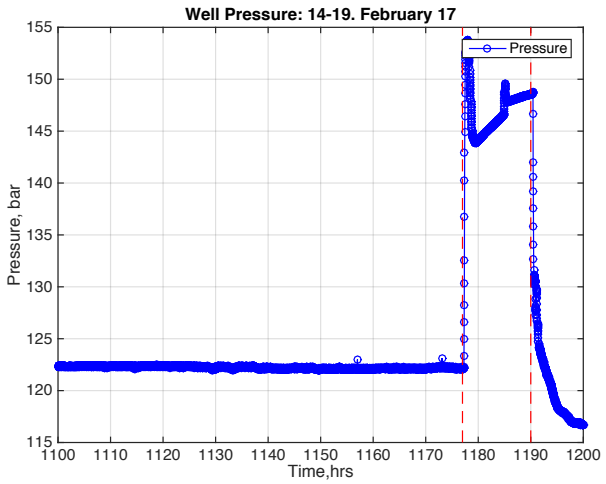

Figure 7.3.5: Measured well pressure 14-19. February 2017.

Figure 7.3.6 on the next page shows measured downhole pressure and estimated bottomhole pressure. The estimate assumes the gas in the production tubing rises rapidly when the well is not producing, such that the production tubing between the bottom of the well and measuring point only contains static liquid. By utilizing the steady-state model, the average density of the liquid phase between the two points is estimated to be 983.2 kg/m^3. The estimate is based on the stationary reference case in table 7.3.1. A liquid density of 983.2 kg/m^3 corresponds to a static pressure difference of 22.2 bars between the measuring point and the perforations.

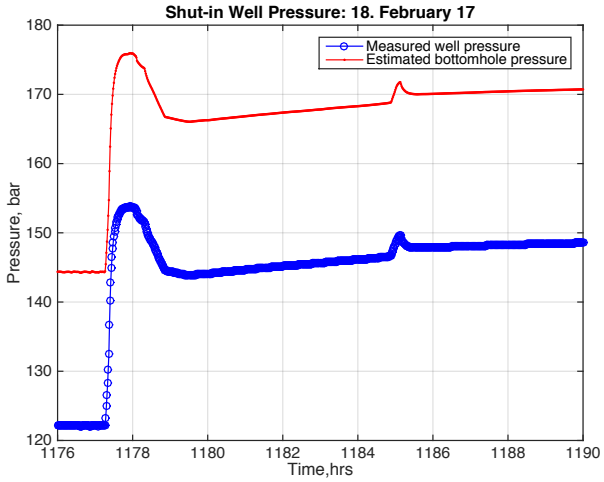

Figure 7.3.6: Measured and estimated well pressure 18. February 2017.

Figure 7.3.6 indicates an initial transient, possibly due to redistribution of gas and liquid in the wellbore. After that, a steady pressure buildup to 171 bars. The estimate is based only on measured pressure data and other simplifying assumptions using the steady-state model. Thus, there is lots of uncertainty in the estimate, and the static reservoir pressure is probably a little higher. Considering the information available it has been determined the estimate is sufficient for further analysis.

7.3.3 Oscillating production

Figure 7.3.1 show several intervals in which the production oscillate and illustrate considerable variation from the mean value. Figure 7.3.7 on the next page shows the production rate as measured in the intervals 28-29. January and 1-2. February, the intervals t = 680-710 and t = 785-805 hours respectively. To better visualize the oscillations only five hours of production 28. January and 1. February has been plotted. The trend of the oscillations, however, remains constant throughout the two intervals mentioned.

The oscillating nature of the liquid rate is obvious, and the amplitudes appear to be rather constant during the periods. The production in the interval t = 680-710 was eventually shut-in for a short time before the well was put on production again. The shutdown was probably due to operational problems and an attempt to control production. Then, a period of stable production follows before the well start to oscillate once again, t = 785-805 hours.

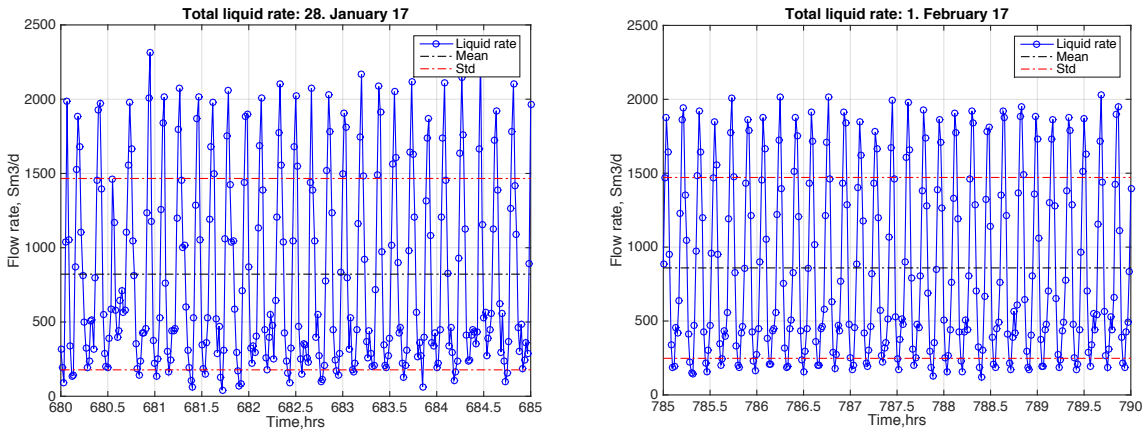

Figure 7.3.7: Oscillating liquid production January-February 2017.

Visual inspection of production 28. January and 1. February 2017 show clear similarities. Although the well was shut-in after the first period the production quickly started to oscillate similarly. Table 7.3.2 below summarize the production characteristics for the two periods. The mean of production increases slightly while the standard deviation decreases.

Table 7.3.2: Production statistics - oscillating production.

Period	**Mean production** $[\mathbf{Sm^3/d}]$	**Std production** $[\mathbf{Sm^3/d}]$
28-29. January 2017	827.0	634.4
1-2. February 2017	858.6	617.9

The standard deviations tell there is a significant variation in the liquid production for both periods. To better examine the oscillations the data have been transformed to the frequency domain using the Fourier Transform. Figure 7.3.8 show the amplitude spectrum of the measured flow rates. The figure show dominant amplitudes of about 483 Sm^3/d and 623 Sm^3/d. Both periods oscillate at equal frequencies, 5.66 hr^{-1}, with a duration of 10.6 minutes.

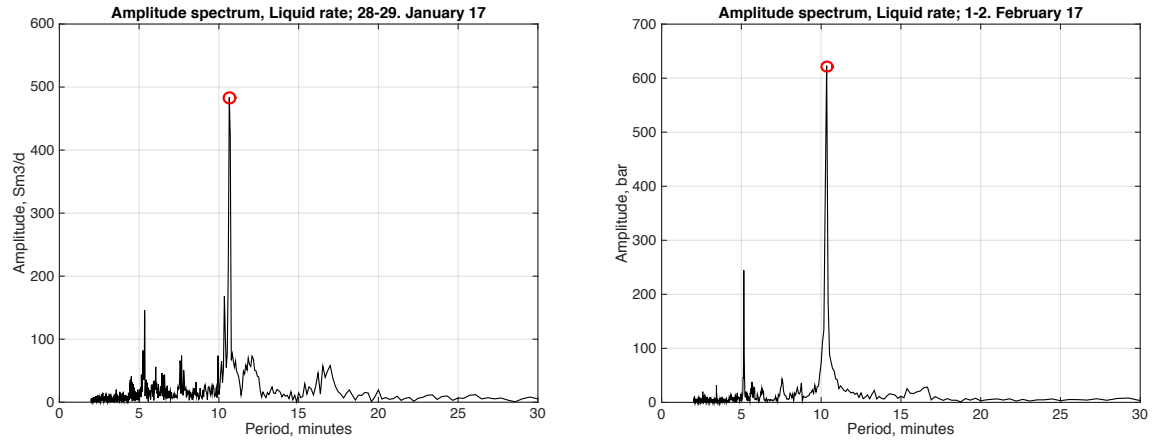

Figure 7.3.8: Amplitude spectrum liquid rates January-February 2017.

For gas lift systems subjected to flow instability, pressures and flow rates usually oscillate at equal frequency, but with some phase-shift. Figure 7.3.9 shows the measured pressure at the wellhead and downhole for five hours 28. January 2017. As for the liquid rate, the pressures seems to oscillate with a rather constant amplitude around the mean.

Figure 7.3.10 shows the pressure amplitude spectrum's 28-20. January and reveal dominant amplitudes of around 7 and 2 bar for the wellhead and downhole pressure respectively. The oscillatory period for both the wellhead and downhole pressure is 10.6 minutes. The same as for the liquid rate, as expected. Investigation of the pressures 1-2. February 2017 show same attributes.

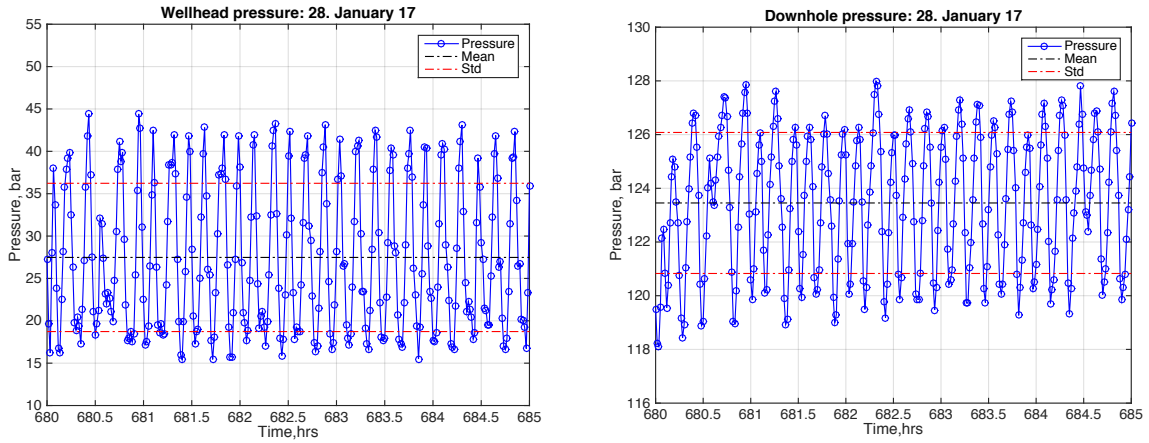

Figure 7.3.9: Downmhole and wellhead pressure oscillations 28. January 2017.

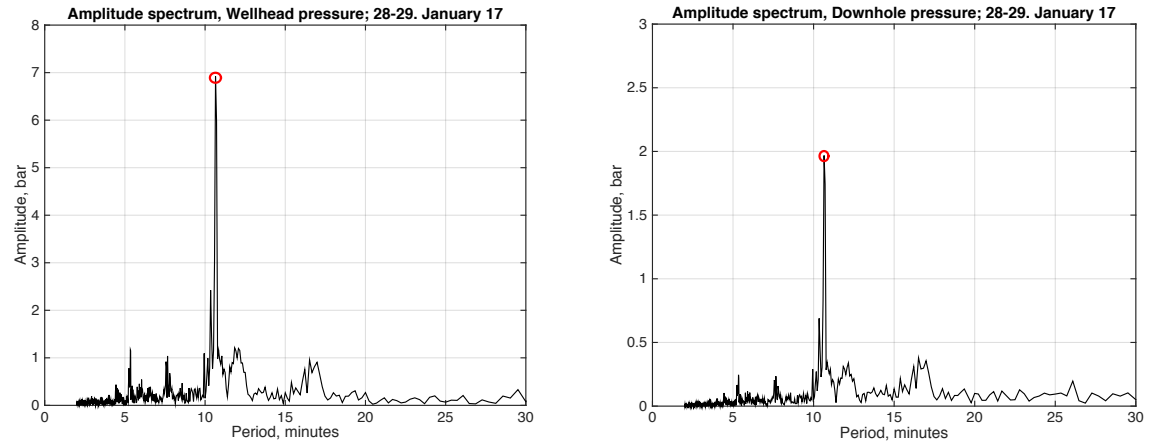

Figure 7.3.10: Amplitude spectrum pressure oscillations 28-29. January 2017.

Rate and pressure variations

The discovery above reveals constant oscillations in both pressure and flow rate when severe flow instability develops. In the two periods investigated the entire gas lift system seems to oscillate at a dominant frequency, affecting both the production rate and pressure in the well. The figures on the next page illustrate rate and pressure variations for the two periods examined.

Figure 7.3.11a and 7.3.12a shows the variations in liquid production and injection rate. Figure 7.3.11b and 7.3.12b shows how the downhole pressure and injection rate varies. Frequency analysis reveals that all rates and pressures oscillate at the same frequency. The oscillation period may also be visualized from the figures, but with phase lags. An interval of two hours has been used to visualize the oscillations better.

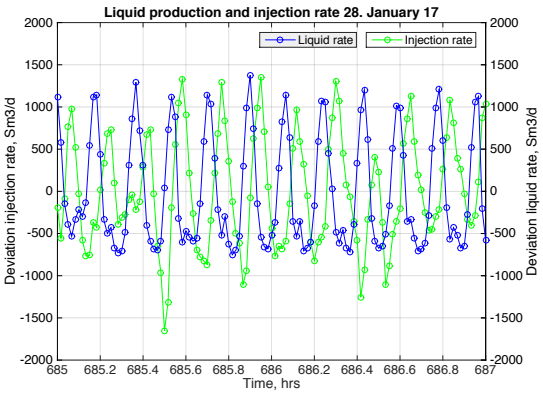

(a) Liquid production and injection rate.

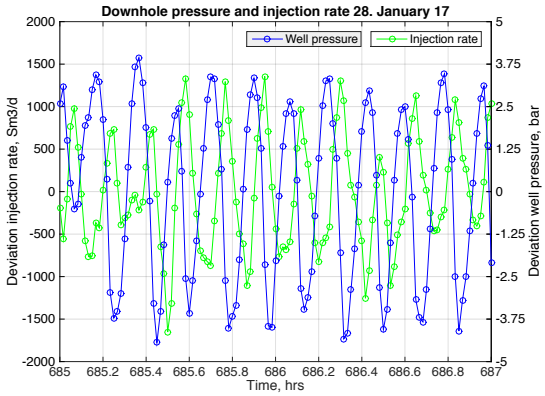

(b) Downhole pressure and injection rate.

Figure 7.3.11: Rate and pressure variations 28. January 2017.

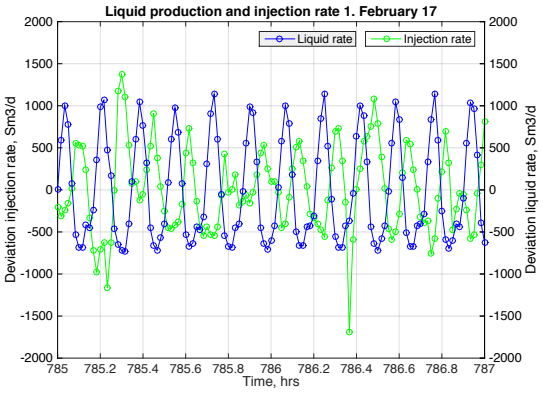

(a) Liquid production and injection rate.

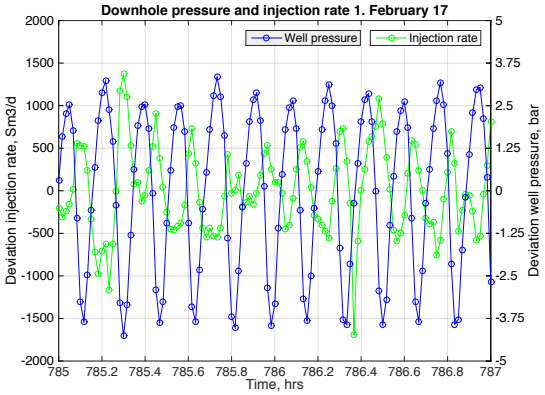

(b) Downhole pressure and injection rate.

Figure 7.3.12: Rate and pressure variations 1. February 2017.

Other periods in January 2017 subjected to oscillations show similar behavior and oscillations of more or less the same frequency present in the measurements.

The length of the production pipe from the injection point is 1826 meters, and the steady-state well model estimates the flow speed to be around 3.4 m/s. The flow time from the inlet to the outlet then becomes, $\Delta t \approx 9$ minutes. Thus, oscillation period is of order-of-magnitude similar to flow time along the tubing. This indicates that the oscillations might be due to the varying inflow of gas-oil ratio, suggesting kinematic waves as an underlying mechanism of the instability (Asheim, 2016).

Dynamic productivity index

When the pressure in the well varies, the inflow of reservoir fluid will also vary. The productivity index, equation 7.3.2, quantifies the dependence of well pressure on the liquid inflow rate.

$$J = \frac{q_l}{p_r - p_{wf}} \tag{7.3.2}$$

However, when pressure and flow rate oscillate around an average, it is more practical to evaluate the pressure-rate dependence by the relationship between the variations, a dynamic productivity index (Asheim, 2000). The dynamic productivity index is defined as the ratio of the change in inflow rate to bottom well pressure. The expression can be derived using Darcy's equation, and it can be shown that the dynamic productivity (at established oscillations) index depend on the frequency, not the amplitude. There will also be a phase shift relative to stationary production. At stationary production, the maximum inflow rate is achieved when the well pressure is at a minimum. At oscillating production, however, maximum production is achieved at maximum well pressure (Asheim, 2000).

If we neglect the phase difference, the dynamic productivity may be approximated as

$$j = \frac{q_l(t) - \bar{q}_l}{p_w(t) - \bar{p}_w} = \frac{\delta q_l}{\delta p_w} \approx \frac{A_{ql}}{A_{pw}} \tag{7.3.3}$$

Where A_{qw} and A_{pw} are the amplitude of the oscillations in flow rate and well pressure, respectively. Substituting in the amplitudes obtained 28-29. January and 1-2. February we get values of around 254 $Sm^3/d/bar$ and 260 $Sm^3/d/bar$. The dynamic productivity index is approximately ten times higher than the stationary productivity index. The magnitude of the productivity index tells us that liquid production responds much stronger to oscillating pressure variations than stationary pressure variations. This may be explained due to fluid expansion/compression around the wellbore.

7.3.4 Well stabilization

Both periods examined above show oscillatory production, separated by an interval that appears to contain stationary production. Figure 7.3.13 shows the production was shut-in for approximately 1 hour following the unstable production 28-29. January 2017.

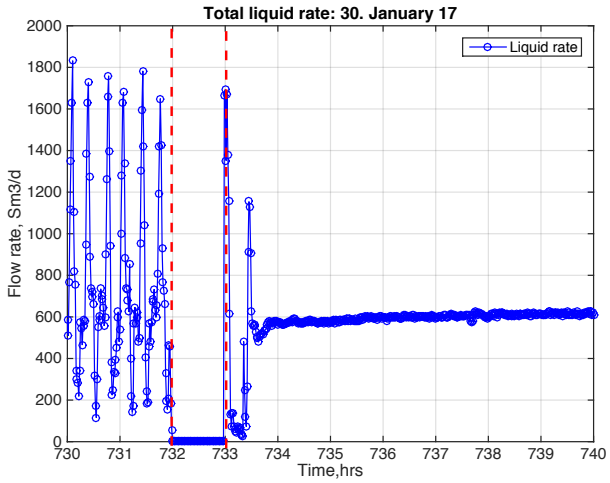

Figure 7.3.13: Liquid production rate 30. January 2017.

When production is resumed, the analysis shows that the well produces stably, comparable to production the first 400 hours at the beginning of the month. Thus, temporary shutdown of production may stabilize the well. After only 35 hours, however, oscillations start again.

7.3.5 Initiation of instability

There might be minor variations and disturbances in the system which later leads to larger oscillations in the tubing. Two different periods, 20-23. March 2016 and 6-9. May 2016, have been inspected to give an explanation to how and why oscillations initiate in the well. In this way, it is ensured that the conditions and dynamics that leads to oscillations are not random, but something that recurs before the instability.

Well production 20-23. March 2016

Figure 7.3.14 and 7.3.14 on the next page shows pressure and production rates 23. March 2016. The plots illustrate how the conditions in the well change when production goes from stable to highly variable. The red line shows an exponential moving average fitted to the data.

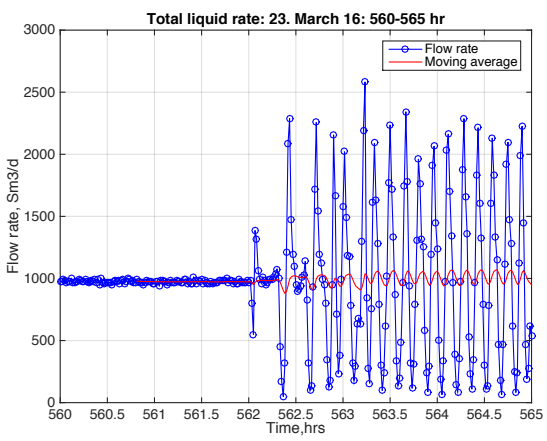

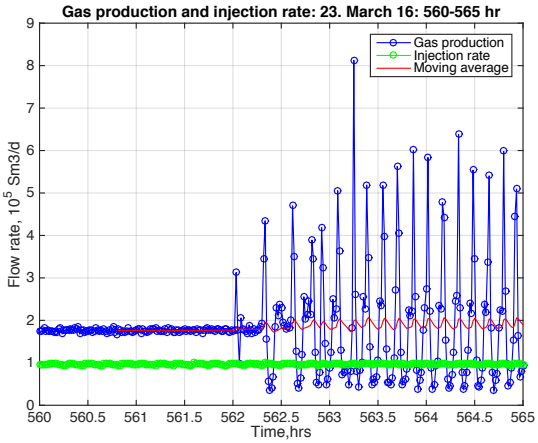

Figure 7.3.14: Liquid production rate and gas production and injection rates 23. March 2016.

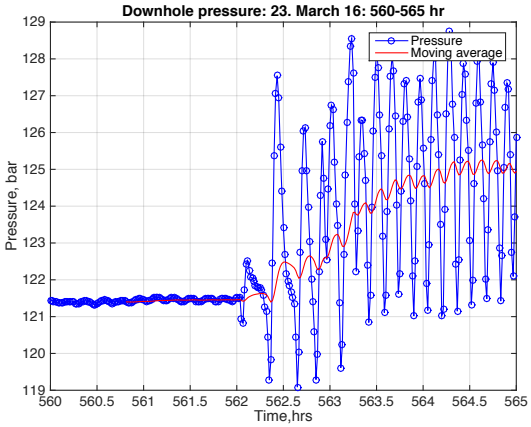

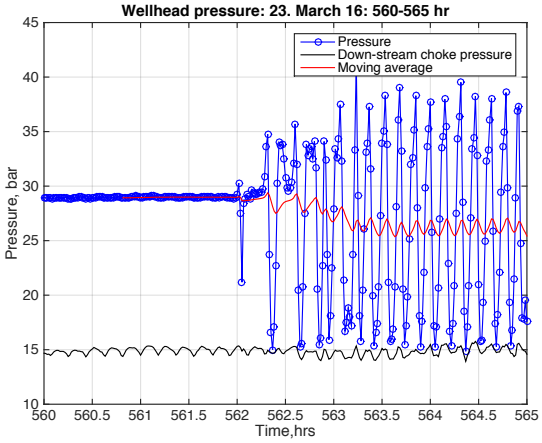

Figure 7.3.15: Downhole and wellhead pressures 23. March 2016.

The moving average captures the change in the mean by giving more weights to the most recent measurements and provide an indication of the trend as the rate and pressure changes. An exponential moving average has been used because it reacts more quickly to changes compared to other moving averages.

Figure 7.3.14 and 7.3.15 show the oscillations are initiated at approximately 562 hours and as the oscillations grow it may be observed that the average well pressure goes up by about 4 bars. The average pressure at the wellhead declines slightly from 29 bars to 26 bars. The moving average of the liquid and gas production rates remain rather constant, but the amplitude of the variations grow large. The data show the conditions change dramatically over a relatively short period. Oscillations seem to be well established after 30 minutes, from 562 to 562.5 hours.

Production history March 2016

To investigate the cause of the emerging oscillations the production history from 20-23 March 2016 has been further examined. Figure 7.3.16 and 7.3.17 show lift-gas delivery pressure at the wellhead, gas injection pressure, liquid rate, and injection rate of lift-gas for the period. Compared to the oscillations observed above, these measurements show less variation and smaller amplitude. At times, however, the amplitudes appear to be somehow constant, and this may suggest that the variations oscillate repetitively.

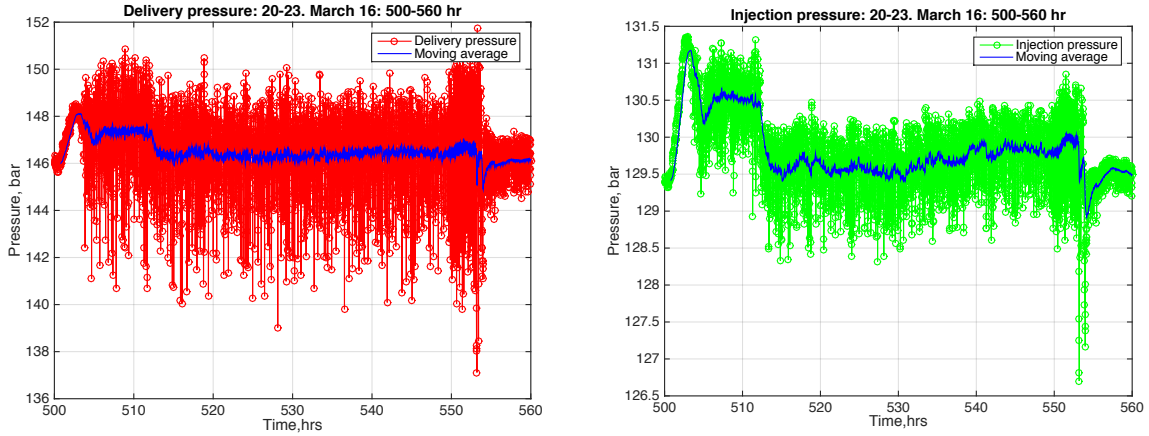

Figure 7.3.16: Gas delivery and injection pressures 20-23. March 2016.

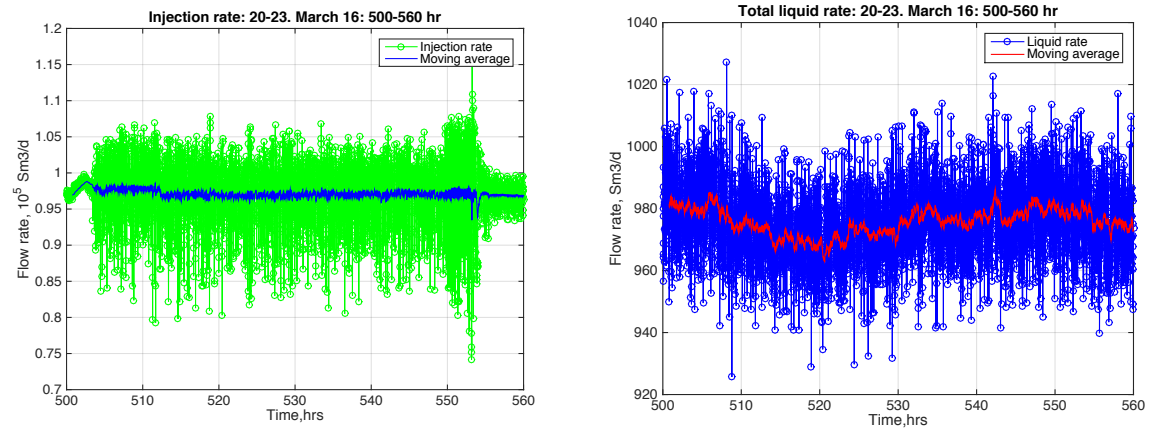

Figure 7.3.17: Gas injection and liquid production rates 20-23. March 2016.

The figures on the next page illustrate the amplitude spectrum's and clarify the variations observed in figure 7.3.16 and 7.3.17. The delivery pressure, injection pressure, and gas injection rate appears to oscillate at the same frequency, with an oscillation period of 12.5 minutes. Although the amplitudes are small, they seem to be consistent. The amplitude of the injection rate is considerably larger than the other amplitudes. This is because the injection rate is in the order of $10^5 Sm^3/d$. The amplitude spectrum of the liquid rate, however, appear more chaotic and shows no stable oscillation frequency.

Even though the injection rate oscillates with a relatively large amplitude, the liquid production still appears more or less stationary at this time.

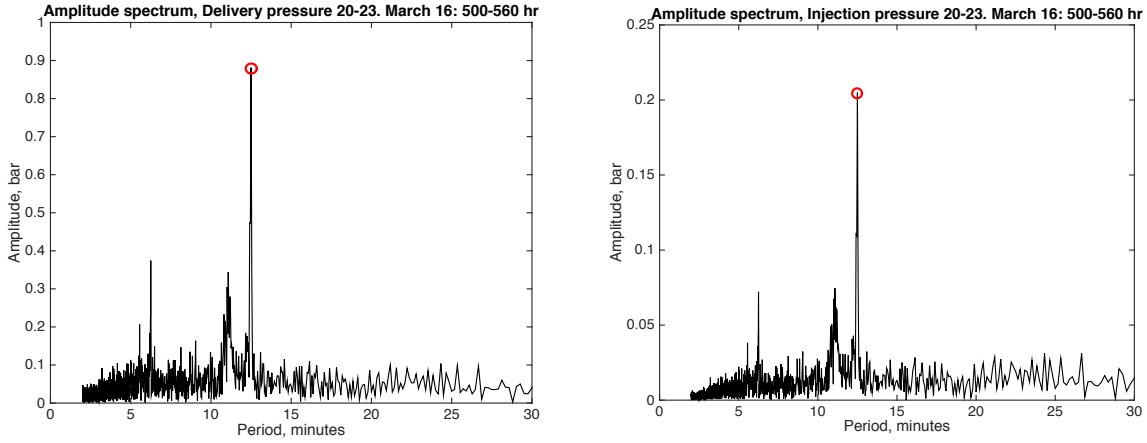

Figure 7.3.18: Amplitude spectrum gas delivery and injection pressures 20-23. March 2016.

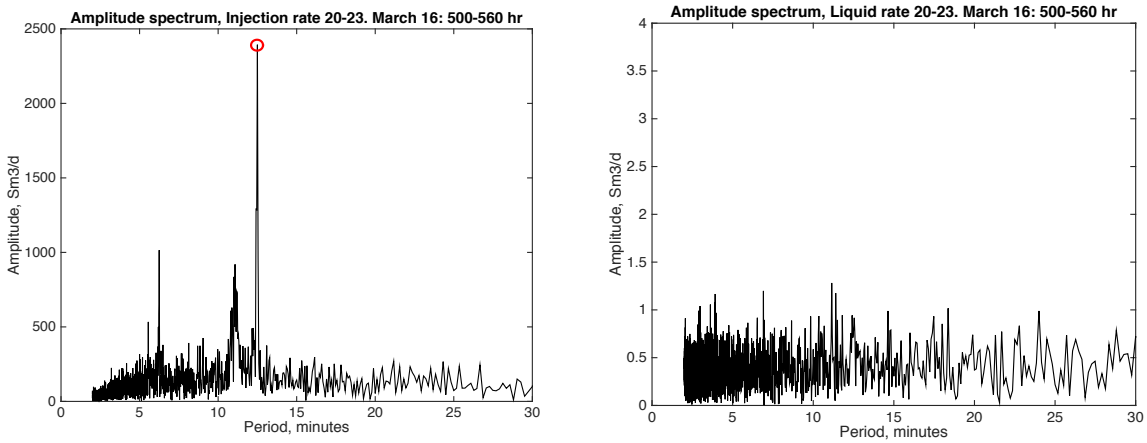

Figure 7.3.19: Amplitude spectrum gas injection and liquid production rates 20-23. March 2016.

Figure 7.3.20 on the next page shows liquid production 23. March ten hours later, t = 570-590 hours. The oscillations seem to be well established and have a period of 9.5 minutes and a dominant amplitude of around 400 Sm^3/d. Examination of the well pressures indicates oscillations of the same frequency.

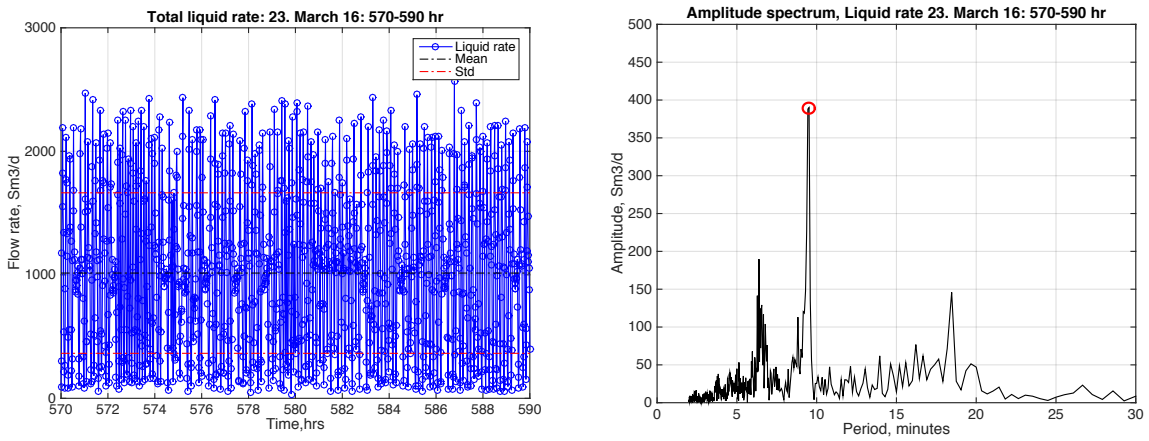

Figure 7.3.20: Oscillating liquid production rate 23. March 2016.

In the period from 20-23. March the gas delivery system show small variations with an oscillation period of 12.5 minutes while the liquid rate shows no stable oscillations. A few hours later, however, the liquid rate develops severe oscillations with a period of 9.5 minutes. The difference in frequency might be due to the characteristics of the system and the erratic nature of the multiphase flow. Although the gas delivery system experiences variations of a particular period it does not necessarily imply the flow in the tubing will develop oscillations of the same frequency. This has to do with the system's natural frequency.

However, the measurements in figure 7.3.16 and 7.3.17 show the variations in the gas delivery system level off just before (around five to ten hours) the oscillations in the tubing develop. Closer analysis of the interval 557-562 hours confirms this. Also, small oscillations in the liquid rate seem to start to develop in this interval. This may indicate that the disturbances observed earlier in the gas delivery system have already initiated smaller flow instabilities before the large oscillations develop.

Well production 6-9. May 2016

The figures on the next page show pressures and production rates 9. May 2016. The conditions in the well show similarities with the measurements observed in March.

The average well pressure goes up by about 8 bars, and the average pressure at the wellhead decline from 23 to 20 bar, analogous to the period in March. The oscillations seem to be established after a relatively short time.

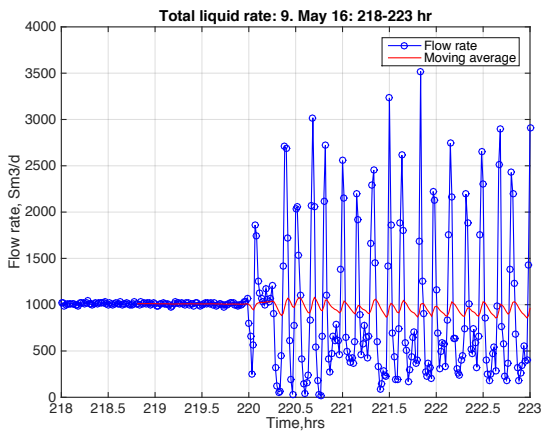

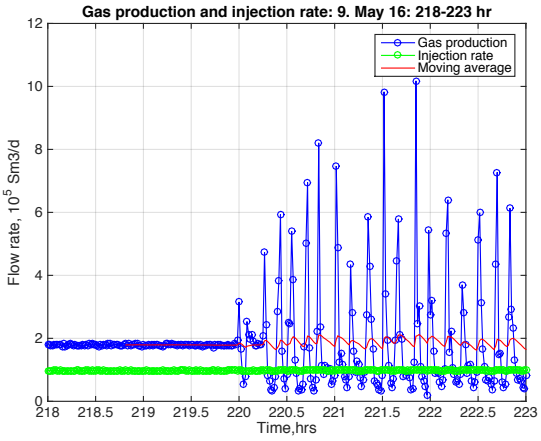

Figure 7.3.21: Liquid production rate and gas production and injection rates 9. May 2016.

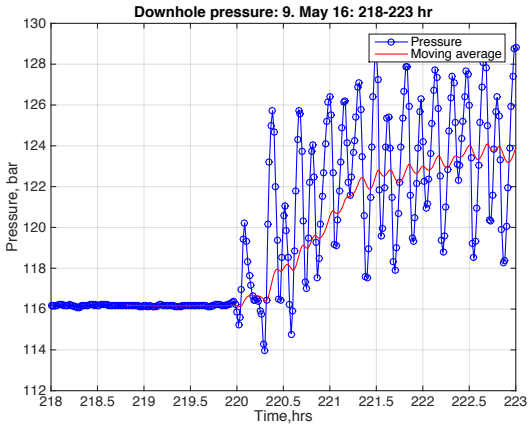

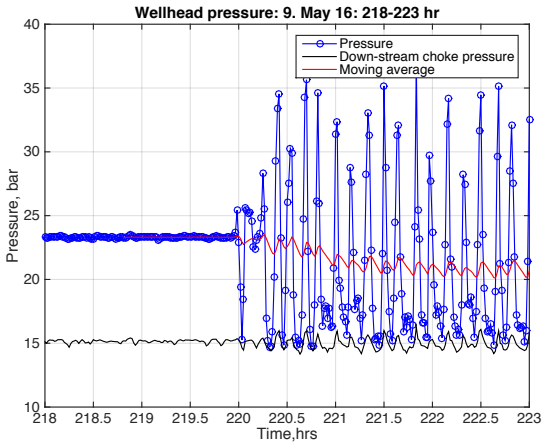

Figure 7.3.22: Downhole and wellhead pressures 9. May 2016.

Production history May 2016

Figure 7.3.23 and 7.3.24 on the next page shows lift-gas delivery pressure at the wellhead, gas injection pressure, liquid rate, and injection rate of lift-gas in the period 6-9. May 2016. Compared to the measurements 20-23. March, the variations appear somewhat smaller and maybe less consistent.

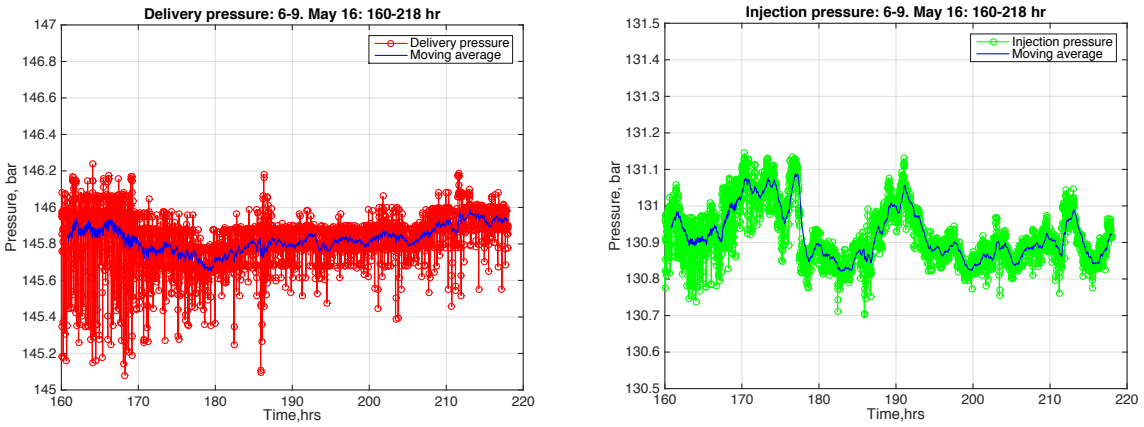

Figure 7.3.23: Gas delivery and injection pressures 6-9. May 2016.

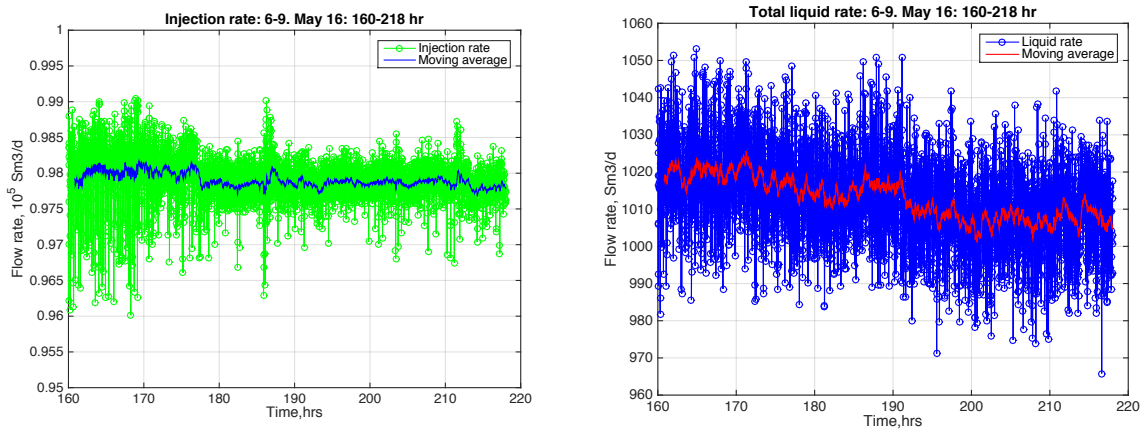

Figure 7.3.24: Gas injection and liquid production rates 6-9. May 2016.

Figure 7.3.25 and 7.3.26 on the next page show the corresponding amplitude spectrum's. The spectrum's show a dominant amplitude at equal frequencies. The oscillation period is estimated to be 13.3 minutes and is slightly higher than for the data examined in March.

An interesting observation can be made from the amplitude spectrum of the liquid production rate. Figure 7.3.24 shows that the liquid rate oscillates at the same dominant frequency as the gas delivery system. This characteristic was not the case for the liquid rate in March and may indicate that the flow in the tubing is more prone to flow instability if the gas delivery system oscillates at lower frequencies.

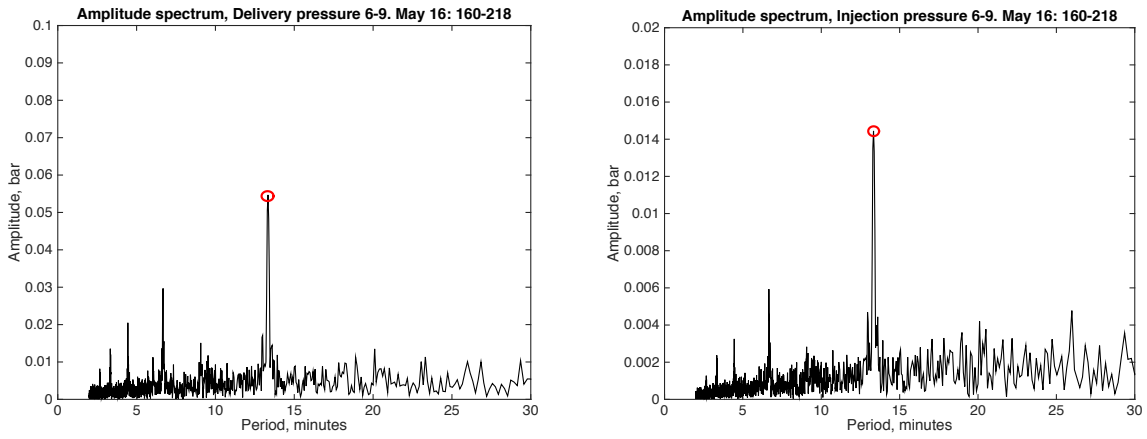

Figure 7.3.25: Amplitude spectrum gas delivery and injection pressures 6-9. May 2016.

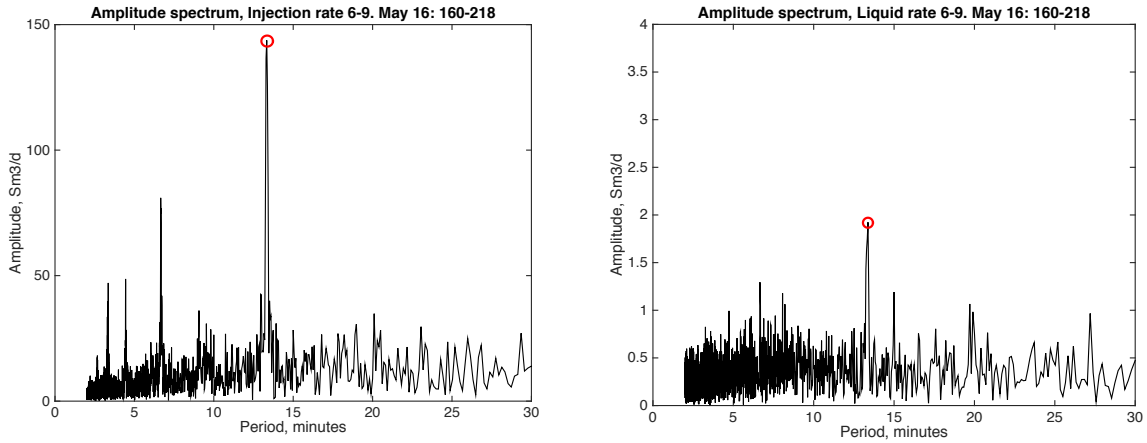

Figure 7.3.26: Amplitude spectrum gas injection and liquid production rates 6-9. May 2016.

Figure 7.3.27 shows liquid production at some hours later 9. May. The oscillations that develop have a dominant amplitude of around 650 Sm^3/d and the oscillation period is estimated to 7.8 minutes. Just before the oscillations develop closer analysis show the variations in the gas delivery system gets smaller and less systematic, similar to what discovered in March.

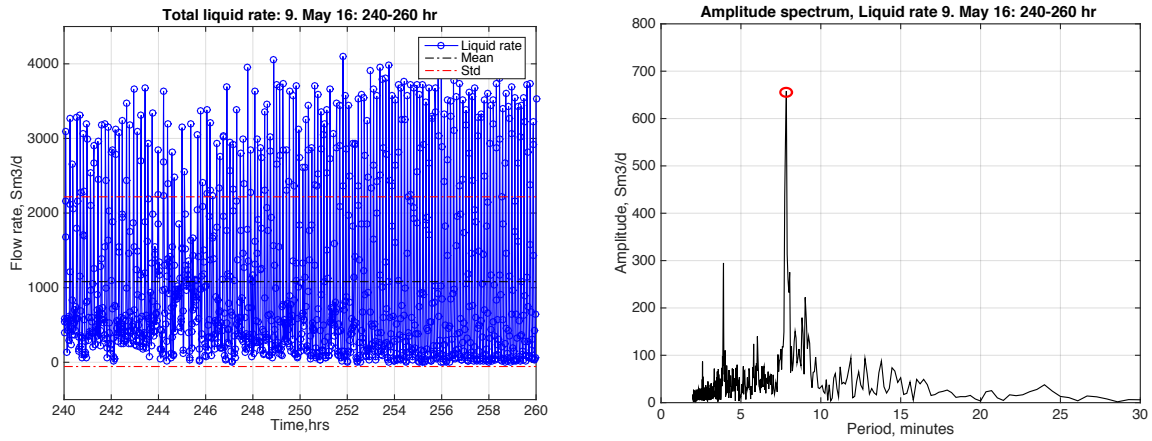

Figure 7.3.27: Oscillating liquid production 9. May 2016

The production in March and May 2016 show similar characteristics ahead of oscillating production. Minor variations in the lift-gas delivery pressure, gas pressure, and injection rate may be a trigger for the oscillations observed in the well. Small variations in the gas delivery system may cause disturbances in the annulus, which affect the injection of lift-gas to the tubing. If these variations are amplified at specific frequencies, this could be an explanation to the instability.

There are, however, some interesting differences in the two periods. Ahead of the instability in March, the gas delivery system oscillates with a period of 12.5 minutes. The liquid oscillations that later develop in the tubing have a dominant amplitude of around 400 Sm^3/d. In May, before the well becomes unstable the gas delivery system and the liquid rate show oscillations with a period of 13.3 minutes. When the well later becomes unstable the liquid oscillations have a dominant amplitude of around 650 Sm^3/d.

The discovery may suggest that the characteristics of the instability observed in the well depend, to some degree, on the history of the gas delivery system. As the gas delivery system oscillates at lower frequencies, the amplitudes that later develop in the tubing are larger.

7.3.6 Diminishing oscillations

The findings in the previous section show periodic variations in the gas delivery system and annulus ahead of larger oscillations in the well. This may indicate the well is prone to instabilities if the well is subjected to small variations/disturbances with period of 12-13 minutes.

In general, the measured flow data show at times short lasting and temporary oscillations. Figure 7.3.28 on the next page shows liquid production 2-17. June 2016. An interesting observation can be made in the interval t = 900-1137 hours. The period show at times small and brief oscillations that cease to exist after only a short period. The behavior seems to be repeating, most evident at 990 and 1030 hours until the variations no longer vanish, but grow into larger oscillations at t = 1137 hours. To gain control of the well the measurements indicate the well was shut-in after 14 hours of oscillating production.

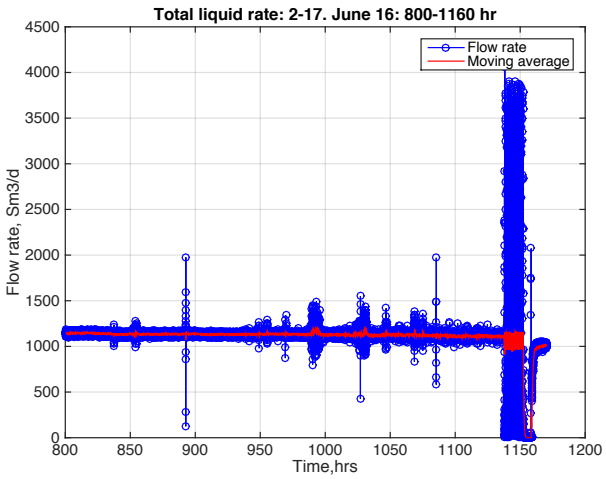

Figure 7.3.28: Liquid production rate 2-17. June 2016.

The figures that follows show the lift-gas delivery pressure at the wellhead, gas injection pressure, liquid rate, and injection rate of lift-gas for 8-10. June, the interval t = 945-985 hours. Compared to figure 7.3.17 and 7.3.16 the variations appear less constant and more scattered around the moving average. Also, visual inspection of the measurements shows the variations have smaller amplitudes than in March and May. Although the measurements do not indicate large fluctuations, there seem to be disturbances in the gas system affecting the delivery and injection of lift gas. Sporadically, the delivery pressure drops in line with the injection rate.

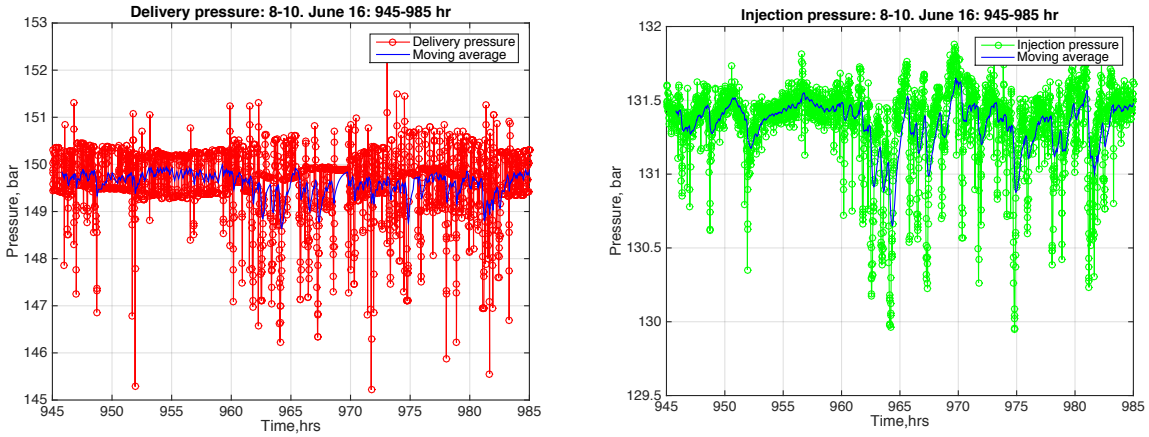

Figure 7.3.29: Gas delivery and injection pressures 8-10. June 2016.

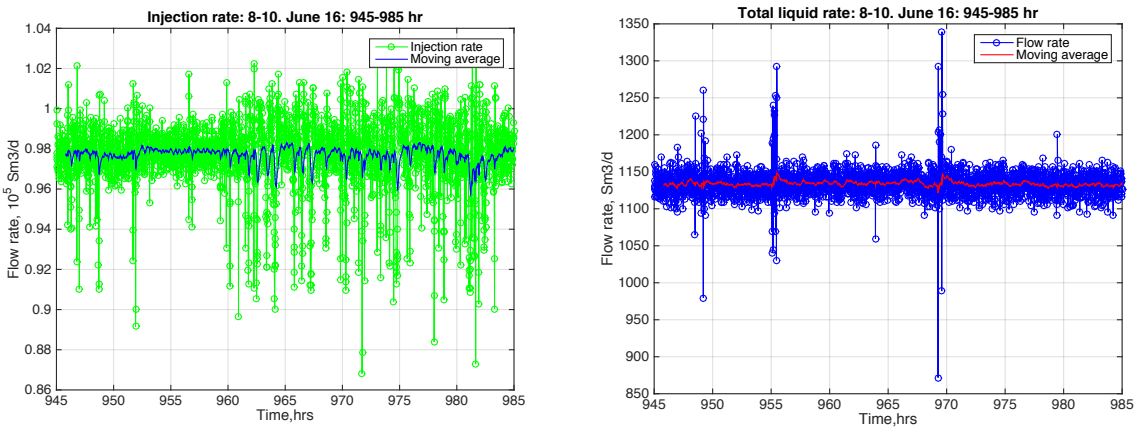

Figure 7.3.30: Gas injection and liquid production rates 8-10. June 2016.

Figure 7.3.31 and 7.3.32 show the associated amplitude spectrum's, prior to the short oscillation cycle at 990 hours. The figures show no particularly clear amplitudes, but it seems to be a dominant amplitude with a period of 23.7 minutes. The amplitude spectrum for the liquid production, however, appear chaotic and with no stable oscillation period. Thus the liquid production still appears random and more or less stationary.

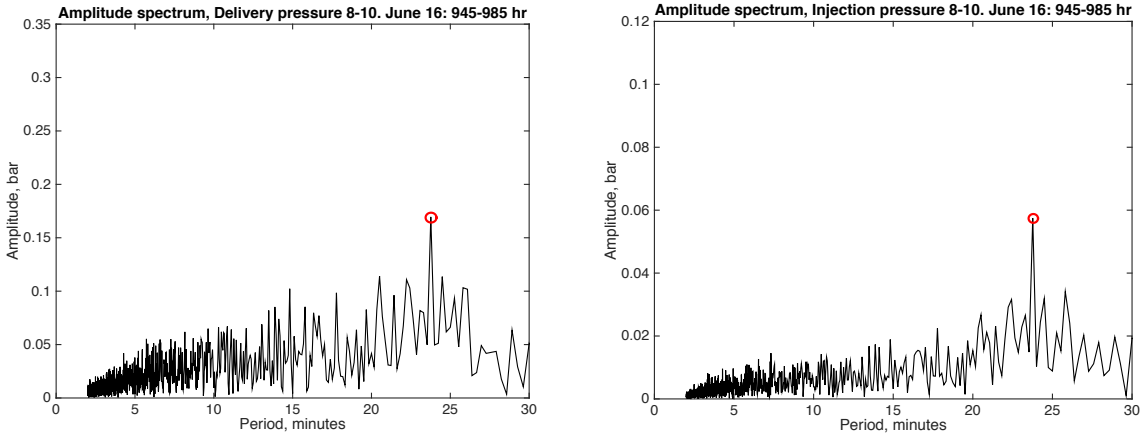

Figure 7.3.31: Amplitude spectrum gas delivery and injection pressures 8-10. June 2016.

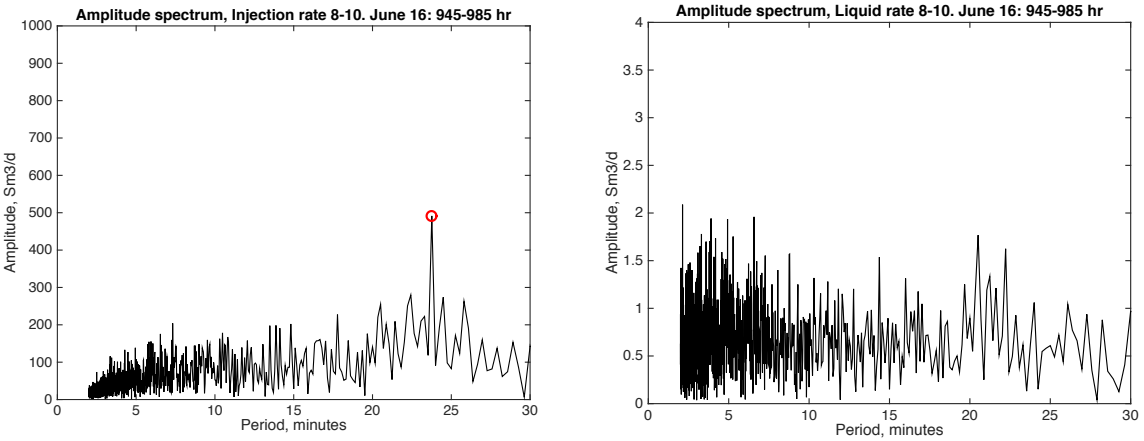

Figure 7.3.32: Amplitude spectrum liquid production and gas injection rates 8-10. June 2016.

Compared to the initiation of larger oscillations (March and May 2016), it turns out the gas delivery system in the period 8-10. June oscillates with a period of 23.7 minutes. Approximately one-half of the oscillation frequency compared to in March and May. The measurements in figure 7.3.28 show the fluid production has a short-lasting oscillation period in the subsequent period t = 990 to 995 hours. A similar response can be observed in the pressure. However, since the response is neither persistent nor leading to greater oscillations, this might indicate the well can oppose disturbances of this characteristics.

Similar behavior may be observed in the subsequent period up to June 16, t = 1137 hours. Alternating intervals of similar response may be detected in the data until large oscillations develop. During the production leading up to the oscillations, the variation in delivery pressure, gas injection pressure, and gas injection rate increases and becomes more established. In a similar fashion as for the intervals examined in March and May the same year.

Chapter 8

Dynamic response study

Periods of unstable production in well 6507/7-A-23 show oscillations with a period of about 8-11 minutes, observed in figure 7.3.8 and 7.3.10. The gas injection rate and reservoir pressure are more or less constant in the periods considered. Still, production rates and pressures show severe oscillations. The analysis in the previous chapter suggests disturbances in the gas delivery system and kinematic waves as possible mechanisms of the instability in the well. The illustrations below show the mechanism for the kinematic wave propagation in the well.

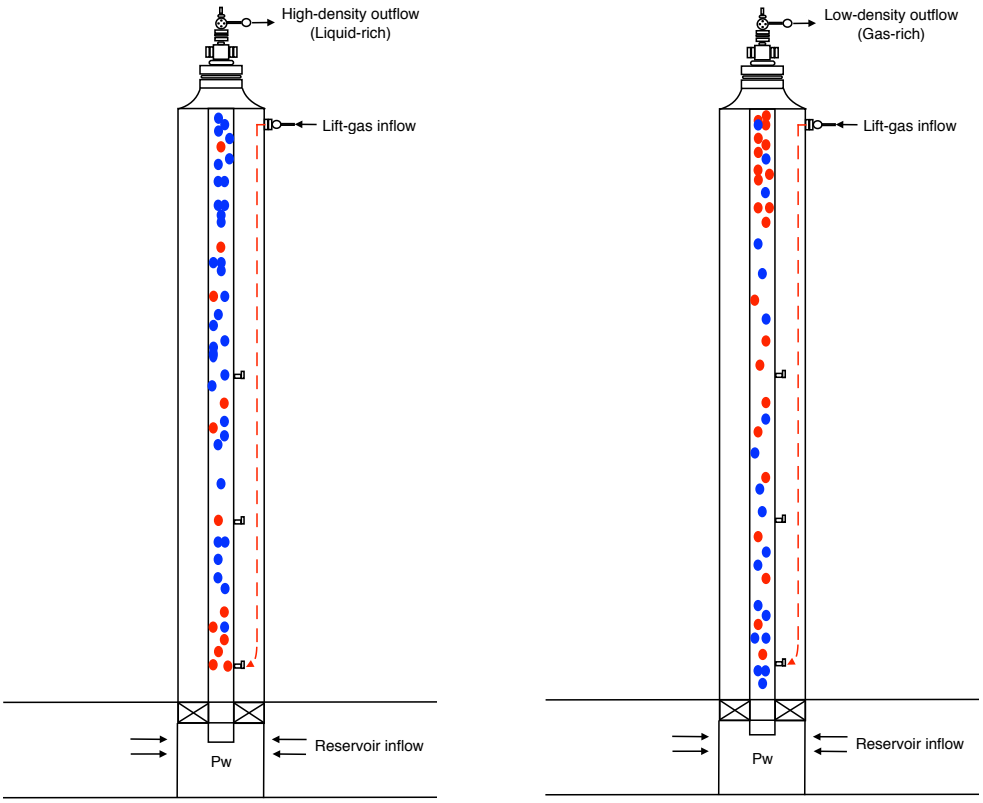

(a) Liquid-rich outflow at time t.

(b) Gas-rich outflow at time t + Δt.

Figure 8.0.1: Mechanism of kinematic waves.

Increased lift-gas inflow to the tubing reduces the density of the fluid mixture. Thus the bottom-hole pressure decreases. At a time later, the fluid mixture of reduced density reach the outlet and will cause the well pressure to increase. A decrease in well pressure, however, will cause a higher inflow of lift-gas. If the delivery pressure of lift-gas at the wellhead is constant, this will cause the pressure in the annulus to decrease. After some time, this will cause the inflow of lift-gas to the tubing to drop. In combination with varying inflow from the reservoir and flow at the outlet, this may amplify the destabilization of the gas lift system (Asheim, 2016).

8.1 Model and prediction

The dynamic response on pressure disturbances may be expressed by the delay-differential equation below.

$$\frac{\vartheta}{\vartheta t}\begin{bmatrix}\delta p_w \\ \delta p_g\end{bmatrix} = \begin{bmatrix}a_1 & -b_1 \\ c & -c\end{bmatrix}\begin{bmatrix}p_w \\ p_g\end{bmatrix}_t - \begin{bmatrix}a_2 & -b_2 \\ 0 & 0\end{bmatrix}\begin{bmatrix}p_w \\ p_g\end{bmatrix}_{t-\Delta t} \tag{8.1.1}$$

Where p_w and p_g are pressure deviations in the tubing and annulus respectively. The kinematic delay between inflow and outflow in the well is expressed by Δt. The model coefficients, a_1, a_2, b_1, b_2, and c relate the dynamic response to fluid and reservoir properties and well design. The parameters may be tuned to investigate the effect of alternative well design and operating conditions. The model may be solved numerically, thus simulating the dynamic response of the well to initial pressure disturbances.

8.2 Numerical simulation for gas lift response

A way of predicting the dynamic response in the well is by numerical simulation of equation 8.1.1 in time. The dynamic response of a well may also be predicted by discretization in time and space such as Hu and Golan (2003) did in OLGA. This approach, however, includes a much more detailed model and will make it harder to interpret the results.

8.2.1 Stable production

The model simulates pressure variations in the production tubing and annular volume at the injection depth. The average of fluid densities and flow rates, from the injection point to outlet, are used in the calculation of the coefficients.

Considering the stationary production interval 1-16. January 2017 (table 8.2.1), linearization around the stationary solution gives the matrix coefficients; $a_1 = -0.000667$, $b_1 = 0.000750$, $a_2 = -0.000846$, $b_2 = 0.000571$, and $c = 0.00130$. The time delay is calculated from the injection depth to outlet and is estimated to be $\Delta t = 6.3$ minutes.

Table 8.2.1: Stationary production 1-16. January 2017

Parameter	
Wellhead pressure, [bar]	22.3
Downhole pressure, [bar]	122.5
Bottomhole pressure, [bar]	138.2
Productivity index, $[Sm^3/d/bar]$	25.0
Oil rate, $[Sm^3/d]$	263.3
Water rate, $[Sm^3/d]$	556.1
Gas rate, $[Sm^3/d]$	1.38 10^5
Injection rate, $[Sm^3/d]$	8.85 10^4
Gas injection pressure wellhead, [bar]	118.9
Injection orifice diameter, [mm]	9.1

Figure 8.2.1 on the next page illustrates the pressure response subjected to an initial disturbance, $\delta p_w = 1$ Pa and $\delta p_g = -1$ Pa. As shown in Chapter 6, the flow rate depends on pressure and will, therefore, show a similar response.

The y-axis shows the simulated pressure deviation from stationary conditions and the x-axis illustrate the time course. The red and blue line represents the annular and tubing pressure response at a depth of the injection valve, respectively. Figure 8.2.1a shows the dynamic response with the time delay neglected (computed with a Runge-Kutta 4th order scheme). Figure 8.2.1b illustrates pressure variations predicted with the delayed response included (computed with Matlab dde23 script). The simulation time is set to two hours to give a better illustration of the initial pressure response. After stabilization, the response remains constant for longer simulation times.

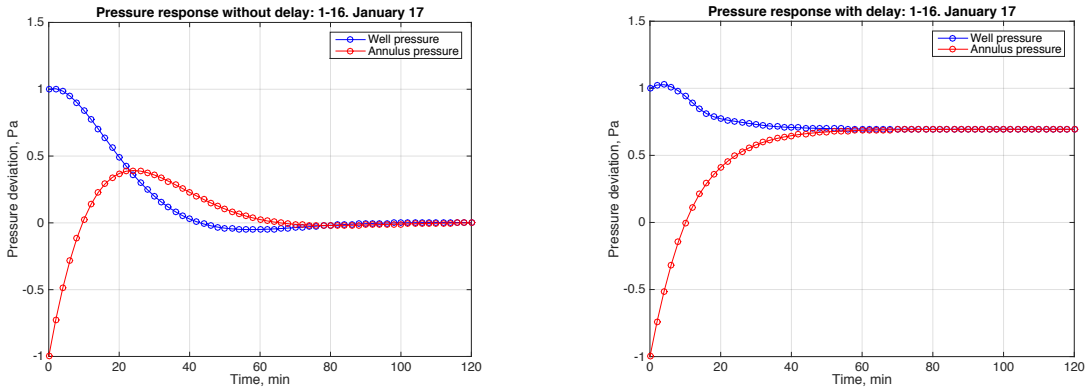

(a) Response without delay.

(b) Pressure response with delay.

Figure 8.2.1: Simulated pressure response for stationary production 1-16. January 2017.

With the delayed response neglected the imposed disturbances decreases with time, and the well appears dynamically stable. The applied disturbances disappear after a short period, and the deviations drop to zero. When incorporating the time delay in the model, the simulation show similar response. However, the deviations stabilize at a value close to the tubing pressure disturbance. The simulation depends on initial conditions, and therefore stabilization will depend on the magnitude of the imposed disturbances. Nevertheless, damped responses like in figure 8.2.1 indicates stability, and this corresponds with the dynamics observed in January 2017.

Assuming a gas-rich fluid mixture reaches the outlet and flows out the tubing. This causes the average density in the production tubing to increase, thus increasing the pressure in the well. If the injection of lift-gas through the orifice is sensitive to tubing pressure, an increase in tubing pressure will cause the injection rate to decrease. This will, in turn, cause the pressure in the annulus to increase. Figure 8.2.2a on the next page shows the response when the annulus and tubing pressure are subjected to the disturbances, $\delta p_w = 10$ Pa and $\delta p_g = 5$ Pa. Only the well pressure is showed to compare the simulated response to the measured well pressure. Figure 8.2.2b shows measured well pressure 1-16 January 2017. The simulation time is set to 400 hours to compare the pressure response with measured data. The pressure response without time delay predicts zero pressure deviations and has not been included.

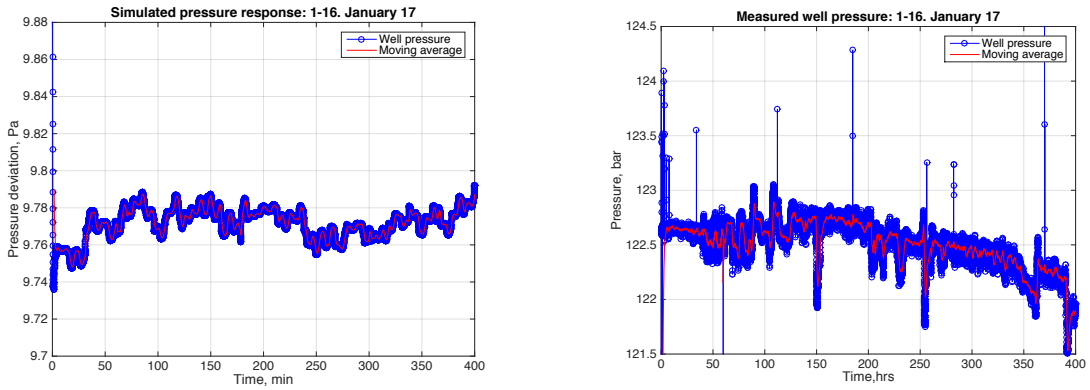

(a) Simulated downhole pressure response.

(b) Measured downhole well pressure.

Figure 8.2.2: Simulated pressure response and measured pressure 1-16. January 2017.

By including the variations at the outlet as in figure 8.2.2a, it seems the well model can capture the dynamics observed in the well at certain initial conditions. Although the simulation indicates persistent pressure oscillations, the variations are so small that production may be regarded as stationary. Applying a positive pressure disturbance to both the tubing and annulus seems to initiate small variations in the pressure. The variations appear more chaotic than systematic, and frequency analysis showed no stable oscillation.

Multiple simulation runs suggest that increasing the magnitude of the disturbances or increasing the simulation time does not cause the variations to increase.

8.2.2 Oscillating production

In an attempt to model oscillating production as observed in the well, production data ahead of the oscillations 28-29. January 2017 have been used as a reference. Figure 8.2.3 on the next page shows measured well pressure 27-29. January the same year. At roughly 680 hours the average well pressure increases from 120 to 123.5 bar. The pressure increase may be due to a sudden density change in the production tubing. Varying inflow and outflow can cause the conditions in the well to change and may help to explain the abrupt increase in tubing pressure.

Investigation of the measured data reveals a stationary production interval, t = 660-678 hours, ahead of oscillating production. Using the stationary interval as an operational reference, it is possible to investigate if the model can replicate the unstable flow behavior.

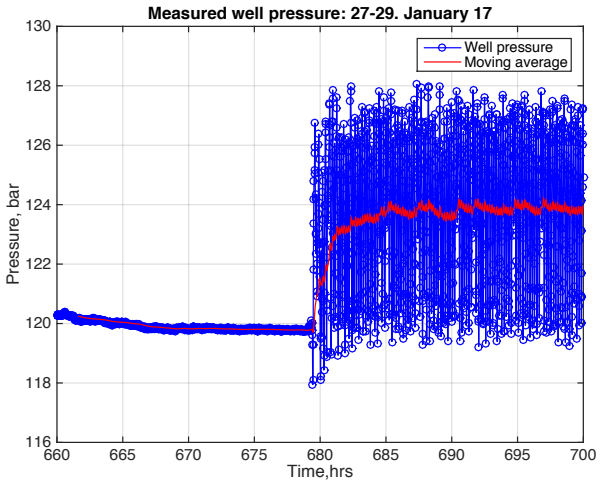

Figure 8.2.3: Measured well pressure 27-29. January 2017.

Considering the stationary gas lift scenario in table 8.2.2 provides the matrix coefficients; a_1 = -0.000610, b_1 = 0.000708, a_2 = -0.000736, b_2 = 0.000583, and c = 0.00110. The time delay is estimated to, $\Delta t = 5.4$ minutes.

Table 8.2.2: Stationary production 27-28. January 2017

Parameter	
Wellhead pressure, [bar]	31.6
Downhole pressure, [bar]	119.9
Bottomhole pressure, [bar]	132.2
Productivity index, $[Sm^3/d/bar]$	25.0
Oil rate, $[Sm^3/d]$	238.5
Water rate, $[Sm^3/d]$	580.7
Gas rate, $[Sm^3/d]$	1.59 10^5
Injection rate, $[Sm^3/d]$	9.73 10^4
Gas injection pressure, [bar]	129.0
Injection orifice diameter, [mm]	9.1

The response predicted by solving the model equation yields similar results as for the stationary production scenario 1-16. January, and appear dynamically stable. Multiple simulations run with different disturbances applied on the system reveals that the model consistently predicts the well stable for the given gas lift scenario. In fact, analysis of various periods leading to oscillatory production results in close to identical model coefficients as for the scenario above, and thus the model anticipate damped pressure responses.

To model pressure oscillations similar to the measured well pressure, an alternative production scenario has been constructed with some adjustments to the production scenario in table 8.2.1. The size of the injection orifice has been increased to 11.5 millimeters and the injection rate decreased to 4.74 10^4 Sm^3/d. Also, the time delay was estimated from the perforations to the outlet, not from the injection valve as earlier. Keeping all other parameters constant, i.e. water cut, gas-oil ratio, and wellhead pressure, the steady-state gas lift model was used to estimate the required production rates to flow the well. The steady-state solution provided the coefficients: $a_1 = 0.0048$, $b_1 = 0.0057$, $a_2 = 0.0020$, $b_2 = 0.0030$, and $c = 0.0068$. The time delay is estimated to, $\Delta t = 16.7$ minutes. Data on the alternative production scenario are located in Appendix B.

Figure 8.2.4 illustrates oscillations of the same order of magnitude (in bar) as measured in the well. The simulated pressure response shows increasing oscillations, and the deviation resembles the measured oscillations in figure 8.2.4. In the simulation, the initial pressure disturbances were set to $\delta p_w = 9$ pascals and $\delta p_g = -9$ pascals. It should be mentioned that the model is not able to limit oscillations as long as the second order terms are neglected in the perturbation analysis. Thus it is not possible to simulate stable oscillation cycles using the model.

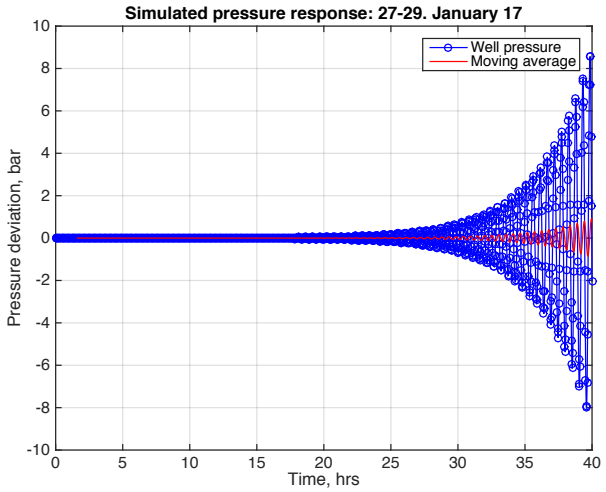

Figure 8.2.4: Simulated pressure response 27-29. January 2017.

Analysis of the oscillating production 28-29. January 2017, section 7.3.3, showed an oscillation period of around 10.6 minutes for pressure and flow rates. The oscillation period predicted by the model equation, however, is around 30 minutes.

The simulations of stable and oscillating production show the dynamic model can recreate the flow dynamics in the well to a certain extent. Initiated at the stationary production reference 1-16. January 2017, the model is able to capture the erratic behavior of the measured well pressure when small pressure disturbances were imposed on the system. To model oscillations that increase with time, however, an alternative production reference is required.

8.3 Parametric sensitivity study on stability

Over recent decades, gas lift stability has been the subject of many studies. Along with simulation studies, stability criteria and theories have provided valuable insight regarding stability of gas lift wells. Parameters recognized to affect stability are gas injection rate, injection orifice size, productivity index, injection depth, tubing size. Among others, Asheim (1988) and Alhanati et al. (1993) showed how the listed parameters influence stability and verified their analytic criteria against reported field data. However, some wells predicted to be stable by existing criteria often turn out unstable in practice. The purpose of the current model is to correct this by including the outflow response. By performing a simulation study, the subsequent sections examine the effect of the above parameters on stability.

To observe a significant change in the model response, simulation results in Chapter 8.2 demonstrated that production parameters had to be changed rather much. The reason for the lack of similarity between simulation and measurements is unknown and difficult to tell. It may be due to errors in measurement data and well design parameters, or due to the model's ability to capture the dynamic pressure response.

However, to investigate the effect of the mentioned parameters adjustments have been made to the stationary production reference 1-16. January 2017. Table 8.3.1 summarizes the stationary gas lift scenario chosen as the base case. The orifice diameter has been increased to from 9.1 to 11.9 mm and the time delay is estimated from the depth of the perforations to the outlet. All other parameters are the same.

Table 8.3.1: Gas lift base case - sensitivity study.

Parameter	
Wellhead pressure, [bar]	22.3
Downhole pressure, [bar]	122.5
Bottom hole pressure, [bar]	138.2
Productivity index, $[Sm^3/d/bar]$	25.0
Oil rate, $[Sm^3/d]$	263.3
Water rate, $[Sm^3/d]$	556.1
Gas rate, $[Sm^3/d]$	1.38 10^5
Injection rate, $[Sm^3/d]$	8.85 10^4
Gas injection pressure at wellhead, [bar]	118.9
Injection orifice diameter, [mm]	11.9

8.3.1 Effect of gas injection rate

Increasing the injection rate may improve stability if the gas lift well is producing near its most efficient point, and attributes mainly two factors. Firstly, increased injection rate causes increased friction loss in the tubing, and this has a dampening effect on instability. The other is that increased flow rate in annulus reduce the delay effect, between inflow and outflow, in the annular volume (Hu and Golan, 2003).

In the current model, only the effect of frictional pressure loss is relevant. The figures that follows gives the simulation results for three different gas injection rates, in which the first corresponds to the base case in table 8.3.1. For the different injection rates the steady-state gas lift model has been used to find the well pressure and the corresponding production rates of oil, water, and gas, assuming the water cut and gas-oil ratio stays the same. The steady-state production data under different gas injection rates are located in Appendix B.

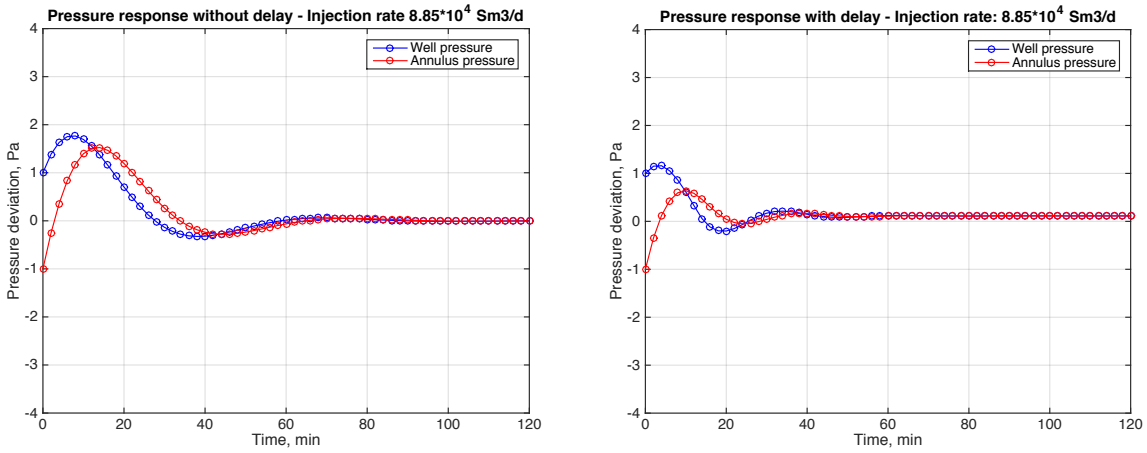

Figure 8.3.1: Dynamic response - Injection rate: 8.85 $10^4 Sm^3/d$.

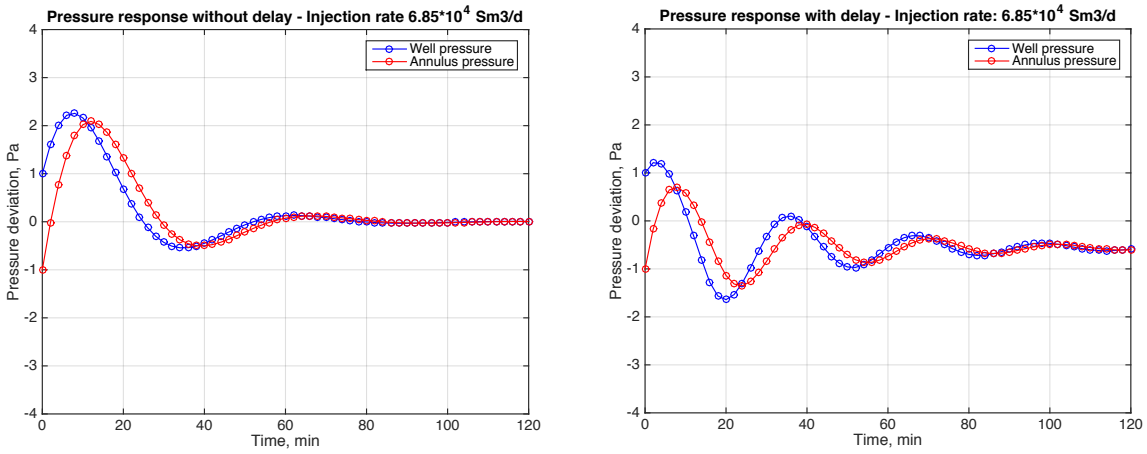

Figure 8.3.2: Dynamic response - Injection rate: 6.85 $10^4 Sm^3/d$.

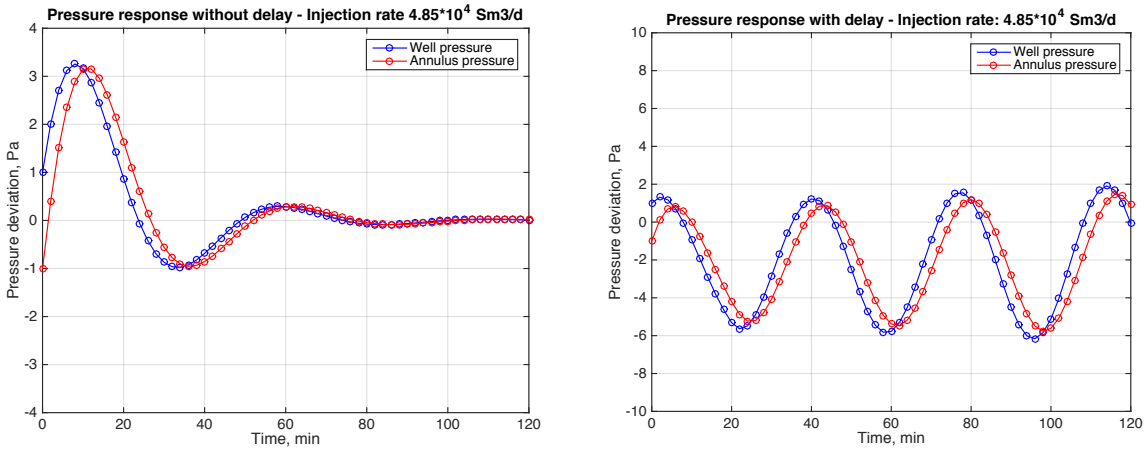

Figure 8.3.3: Dynamic response - Injection rate: 4.85 $10^4 Sm^3/d$.

The first case, figure 8.3.1, has the highest injection rate. It shows the disturbances decreases with time both with and without the time delay included. The well is stabilized at this injection rate. Figure 8.3.2 shows the case when the injection rate is 6.85 $10^4 Sm^3/d$, reduced by around 25 %. Without delay, the initial amplitude increases slightly before the response is stabilized. With the time delay included, damped oscillations emerge, and the effect of decreasing the injection rate is clear. The well, however, still appear stabilized.

Figure 8.3.3 shows the case with the lowest injection rate, 4.85 $10^4 Sm^3/d$. With the delay term included, the applied disturbances lead to oscillations that increase with time, and the system appears dynamically unstable. The oscillation period is estimated to 37 minutes. Without the time delay included the response is approximately as for the cases with higher gas injection rates.

8.3.2 Effect of gas lift orifice size

The orifice size of the downhole injection valve has a strong impact on stability in gas lift wells. Injection valves of smaller orifice diameter promote well stability since it can suppress large flow variations. The effect of orifice size on stability is well documented, and proper valve design is crucial for the operation.

Figure 8.3.1 on the previous page shows the simulation of the gas lift base case with an orifice size of 11.9 millimeters. Figure 8.3.4 and 8.3.5 on the next page shows the pressure response for two cases with different orifice sizes, 9.5 and 14.3 millimeters respectively.

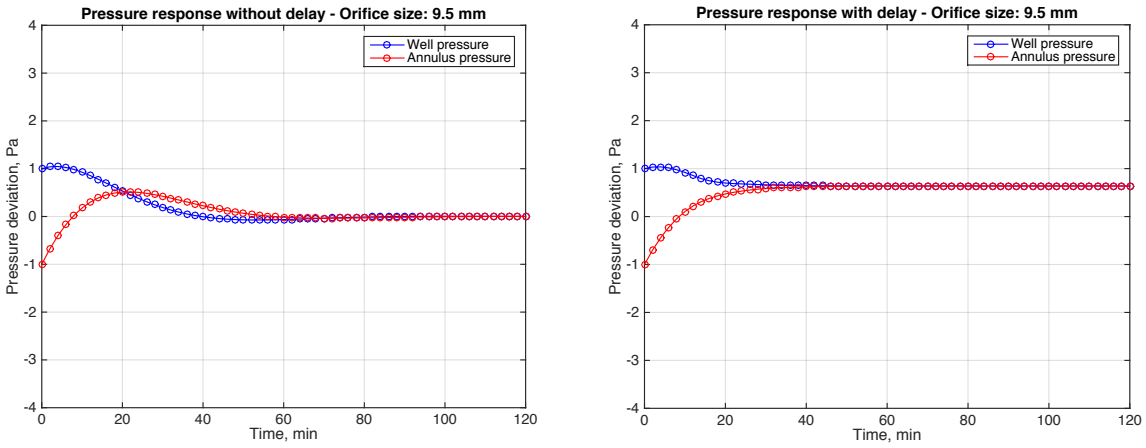

Figure 8.3.4: Dynamic response - Injection orifice size: 9.5 mm.

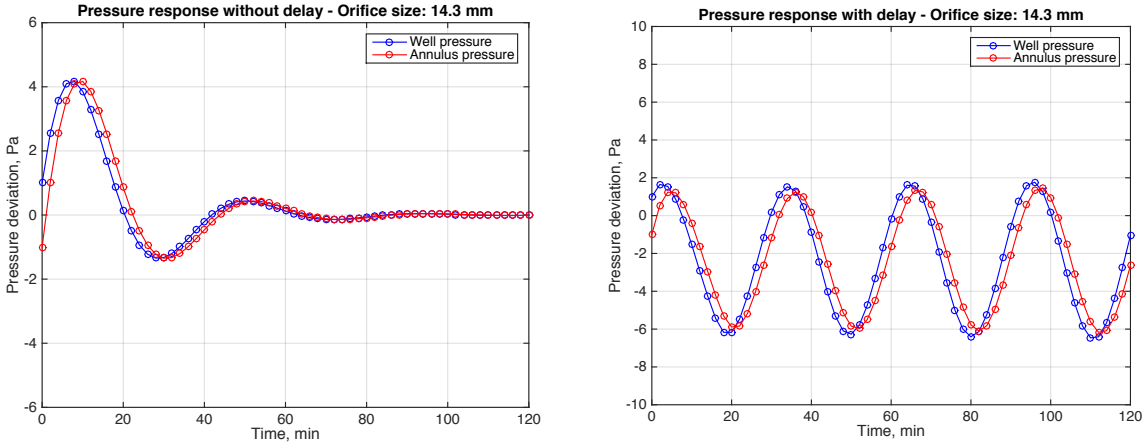

Figure 8.3.5: Dynamic response - Injection orifice size: 14.3 mm.

It is clear that the oscillations are decreased when a smaller orifice size is used in the well. Using an orifice size of 9.5 millimeters, the response with and without time delay is more or less identical. For the case with an orifice size of 14.3 millimeters, there is a big difference in the response. By including the variations at the outflow, an increase in orifice size causes increasing oscillations to develop, and the model predicts the well dynamically unstable.

8.3.3 Effect of productivity index

The productivity index also affects the stability of gas lift wells, and this is quantified by criterion F_1, derived by Asheim (1988). Injection of lift gas to tubing decrease the hydrostatic pressure drop and promote flow instability. A high productivity index introduces more reservoir fluid to the well and increase the average density of the flowing fluid mixture. This will increase the pressure in the tubing and compensate for the increased gas fraction and should stabilize the flow (Asheim, 1988).

The figures below shows the pressure response for a productivity index of 45 $Sm^3/d/bar$ and 5 $Sm^3/d/bar$. The steady-state gas lift model has been used to estimate downhole pressures and flow rates for the different cases. The injection rate and wellhead pressure are the same as for the base case scenario. Production data on the different cases are located in Appendix B.

Figure 8.3.6 shows the case for a productivity index of 45 $Sm^3/d/bar$. The response, with and without delay, seems very similar to the simulation of the base case in figure 8.3.1. Figure 8.3.7 shows the simulation results for a productivity index of 5 $Sm^3/d/bar$.

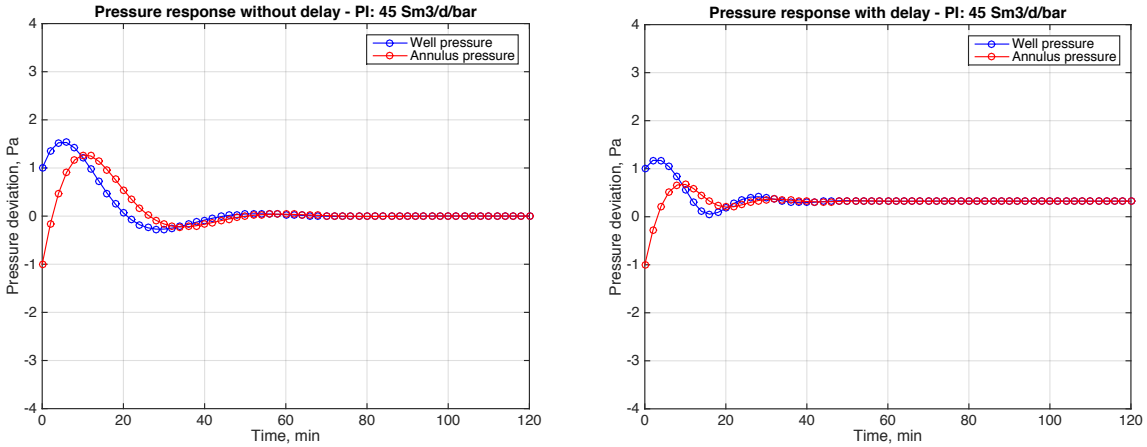

Figure 8.3.6: Dynamic response - Productivity index: 45 $Sm^3/d/bar$.

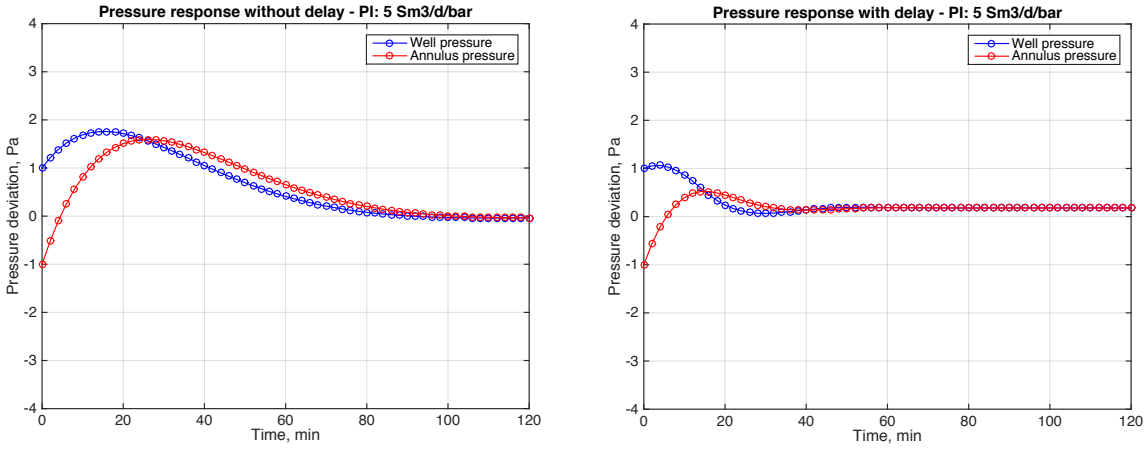

Figure 8.3.7: Dynamic response - Productivity index: 5 $Sm^3/d/bar$.

A smaller productivity index should, according to literature, destabilize the system, but this does not appear to be the case. By including the outflow variations, the response looks more or less identical to the case for a productivity index of 25 and 45 $Sm^3/d/bar$. Without the delay term incorporated in the model, the response also looks similar to the two other cases. The initial amplitudes decrease slightly less with time, but the system still appears dynamically stable.

Multiple simulations with various values of productivity index and injection rates confirm the response observed above. Thus it seems the suggested model is not particularly sensitive to the reservoir inflow.

8.3.4 Effect of injection depth

The effect of the injection depth on stability is illustrated in the figures below. Increasing the depth of the injection point from 1826 (base case) to 2164 and 2850 meters MD destabilizes the system, and may cause the well to be unstable under certain conditions. This should be accounted for when designing a gas lift well. In general, increasing the depth of the injection point boosts the efficiency of the gas lift operation. However, the engineer should always verify if the well is capable of producing without experiencing oscillations with the selected depth of the injection valve.

Figure 8.3.8 and 8.3.9 shows the current model is capable of capturing the effect of the injection depth. For an injection depth of 2850 meters (figure 8.3.9) damped oscillations develop and the well still appear stable. However, the analysis shows that a slight decrease in the injection rate causes the well to experience oscillations that increase with time at this depth. Without time delay, the effect of injection depth is hardly noticeable.

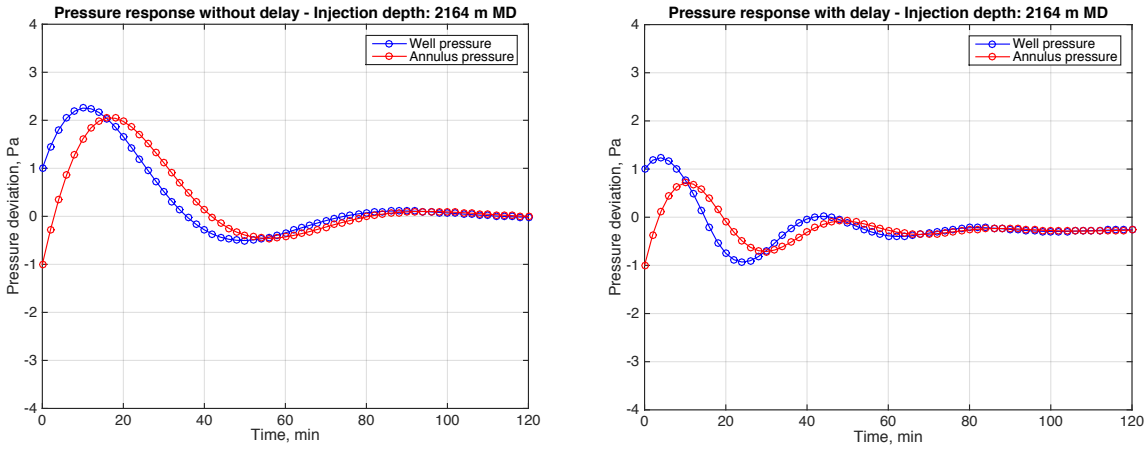

Figure 8.3.8: Dynamic response - Injection depth: 2164 m MD.

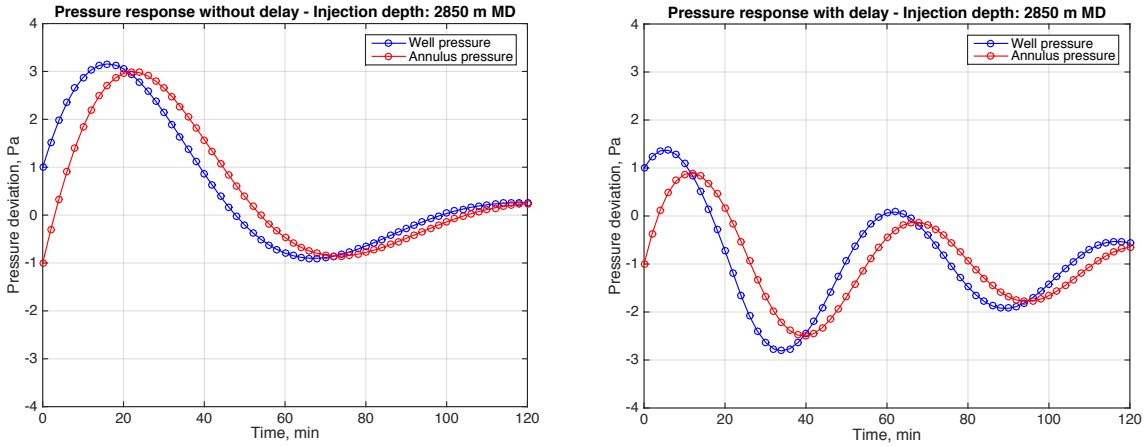

Figure 8.3.9: Dynamic response - Injection depth: 2850 m MD.

8.3.5 Effect of tubing size

Already in the 1950s, Bertuzzi et al. (1953) demonstrated that a decrease in the annular volume might help stabilize gas lift wells. Since then, several studies have investigated and verified the effect of tubing/casing size on stability. To quantify the influence of tubing size on stability the oscillating production scenario in figure 8.3.3 has been used as the base case. Figure 8.3.10 and 8.3.11 demonstrate the effect of changing the tubing size from 6 5/8" (base case) to 5.5" and 7", respectively.

For a tubing size of 5.5" outer diameter, the annular volume is increased, and simulation shows the well is further destabilized. By including the outflow variations, the oscillations increase more rapidly with time and the amplitude of the oscillations increase. When the outflow is not incorporated in the model simulation shows pressure oscillations that decrease with time. Figure 8.3.11 shows that using a 7" outer diameter tubing has a strong stabilizing effect on the well. For a 7" tubing the annular volume is reduced and the model predicts minor oscillations that decrease with time when the outflow is included.

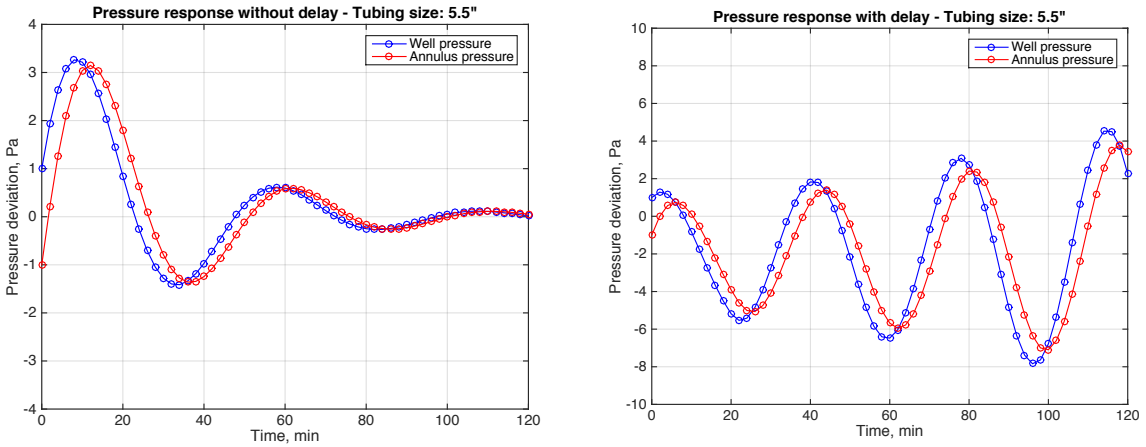

Figure 8.3.10: Dynamic response - Tubing size: 5.5".

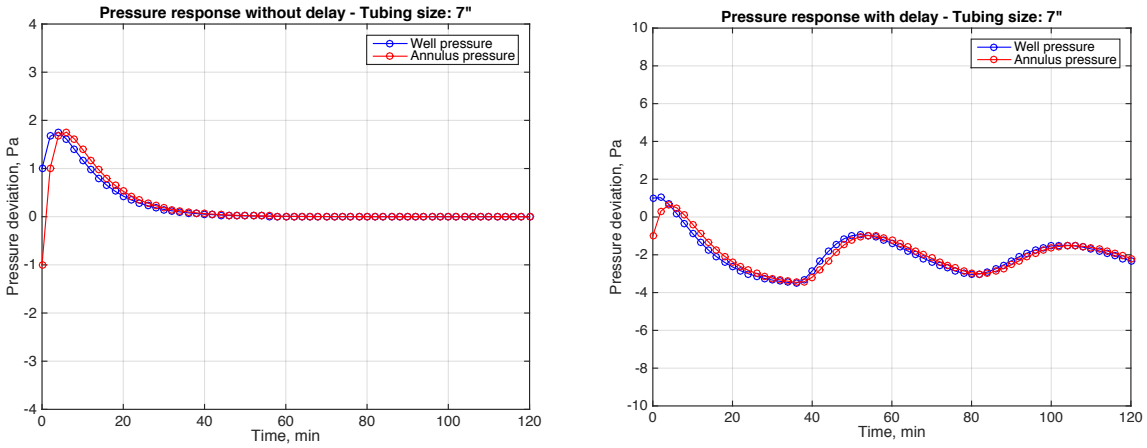

Figure 8.3.11: Dynamic response - Tubing size: 7".

8.4 Analytical solution for gas lift model response

The structure of equation 8.1.1 as well as observed and simulated gas lift instability indicate cyclic and/or exponential responses. In addition to simulation, solutions for the tubing and annular pressures may be expressed as complex exponential functions, but with different amplitude and some phase delay. The solutions may be expressed as $\delta p_w = \hat{P}_w e^{(\alpha+i\omega)t}$ and $\delta p_g = \hat{P}_g e^{\alpha t} e^{i(\omega t+\varphi)}$. Where $\hat{P}_w$ and $\hat{P}_g$ are the initial amplitudes, α is the attenuation factor, $\omega = 2\pi f$ is the oscillation frequency, and φ is the phase delay. Using trigonometric identities the expressions may be rewritten as

$$\delta p_w = \hat{P}_w e^{(\alpha+i\omega)t} = \hat{P}_w e^{\alpha t} \left(cos(\omega t) + isin(\omega t)\right). \tag{8.4.1}$$

$$\delta p_g = \hat{P}_g e^{\alpha t} e^{i(\omega t+\varphi)} = \hat{P}_g e^{\alpha t} \left(cos(\omega t+\varphi) + isin(\omega t+\varphi)\right). \tag{8.4.2}$$

Substituting equation 8.4.1 and 8.4.2 into equation 8.1.1 we obtain after separating real and imaginary components,

$$\begin{aligned} &\hat{P}_w \left[\alpha cos(\omega t) - \omega sin(\omega t) - a_1 cos(\omega t) + a_2 e^{-\Delta t\alpha} cos(\omega(t-\Delta t)\right] \\ &+ \hat{P}_g \left[b_1 cos((\omega t)+\varphi) b_2 e^{-\Delta t\alpha} cos(\omega(t-\Delta t)+\varphi)\right] = 0. \end{aligned} \tag{8.4.3}$$

$$\begin{aligned} &\hat{P}_w \left[\alpha sin(\omega t) + \omega cos(\omega t) - a_1 sin(\omega t) + a_2 e^{-\Delta t\alpha} sin(\omega(t-\Delta t)\right] \\ &+ \hat{P}_g \left[b_1 sin((\omega t)+\varphi) b_2 e^{-\Delta t\alpha} sin(\omega(t-\Delta t)+\varphi)\right] = 0. \end{aligned} \tag{8.4.4}$$

$$\hat{P}_g \left[\alpha cos(\omega t+\varphi) - \omega sin(\omega t+\varphi) + cos(\omega t+\varphi)c\right] - c\hat{P}_w cos(\omega t) = 0. \tag{8.4.5}$$

$$\hat{P}_g \left[\alpha sin(\omega t+\varphi) - \omega cos(\omega t+\varphi) + sin(\omega t+\varphi)c\right] - c\hat{P}_w sin(\omega t) = 0. \tag{8.4.6}$$

From the above expressions follows that the pressure response may exhibit oscillations at harmonic frequencies. If the attenuation factor is positive, the variations will increase with time, and the system may be considered unstable. If the attenuation factor is negative, however, the oscillations decrease with time, such that the system may be regarded as stable. With linearization around a steady-state solution of the gas lift system equation 8.4.3 through 8.4.6 results in four equations and four unknowns, α, ω, φ, and t.

The system of equations may be solved iteratively by considering various initial guesses of the unknowns and different ratios of the initial amplitudes. Investigating the deviation from steady-state production the well and annular pressure may be expressed as

$$p_w(t) = \bar{p_w} + \hat{P}_w e^{(\alpha+i\omega)t}. \tag{8.4.7}$$

$$p_g(t) = \bar{p_g} + \hat{P}_g e^{\alpha t} e^{i(\omega t+\varphi)}. \tag{8.4.8}$$

Where $\bar{p_w}$ and $\bar{p_g}$ are the steady-state tubing and annular pressures respectively.

8.4.1 Stable production

Initiated at stationary production January 2017, the simulations predicted the pressure response dynamically stable, and the applied disturbances quickly vanished. Figure 8.4.1 on the next page shows the response predicted by the analytical solution of the model equation for initial amplitudes of $\hat{P}_w$ = 1 Pa and $\hat{P}_g$ = 1 Pa. The pressure response is estimated by plotting the real part of equation 8.4.1 and 8.4.1. To solve the system of equations the built in Matlab function fsolve was utilized.

Table 8.4.1 summarizes the dynamic parameters from the analytical prediction. The table also shows the parameters change when the initial amplitude of the tubing pressure is increased to $\hat{P}_w$ = 2 Pa. Increasing the amplitude ratio, $\hat{P}_w/\hat{P}_g$, from 1 to 2 seems to drive both the attenuation factor, angular frequency, and phase lag towards zero.

Table 8.4.1: Dynamic parameters for analytical solution - stable production.

$\hat{\mathbf{P}}_\mathbf{w}/\hat{\mathbf{P}}_\mathbf{g}$ [-]	**Atten.fac. [1/s]**	**Angular freq. [1/s]**	**Phase lag [rad/s]**
1/1	-0.0004	0.0009	-0.8942
2/1	-0.0001	0.0005	-0.7109

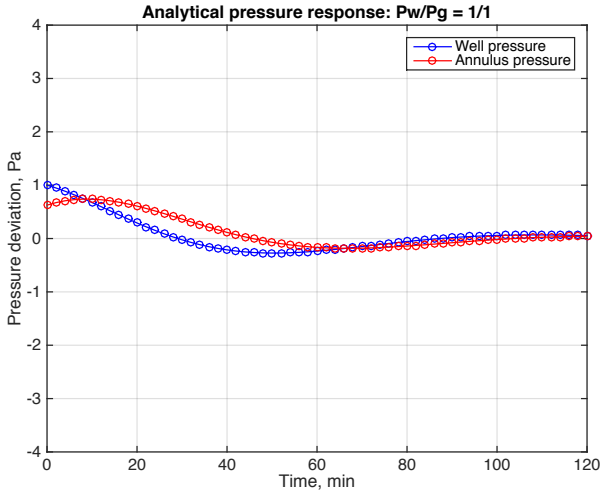

Figure 8.4.1: Analytical pressure response for stable production: $\hat{P}_w$ = 1 Pa, $\hat{P}_g$ = 1 Pa.

Figure 8.4.1 shows similar response to what was predicted by the simulations in Chapter 8.2.1. Solving the analytical solution gives negative attenuation factors, and thus the system may be considered dynamically stable. The initial amplitudes level off quickly and become apparently constant after 60 minutes. So, the analytical solution confirms that the system is damped as predicted by simulation of stationary production 1-16. January 2017.

Figure 8.4.2 shows the solution when the amplitude ratio is increased to 2/1. The solution confirms that the system is stable. However, the time for the amplitudes to level off is considerably longer, and the variations become constant after approximately 500 minutes. Increasing the amplitude ratio further causes the pressures to stabilize immediately at their initial amplitude value as if the system stabilizes at another stable steady-state. Decreasing the amplitude ratio to $\hat{P}_w/\hat{P}_g$ = 1/2, however, causes the amplitudes to decline more rapidly, and the system appears strongly stabilized.

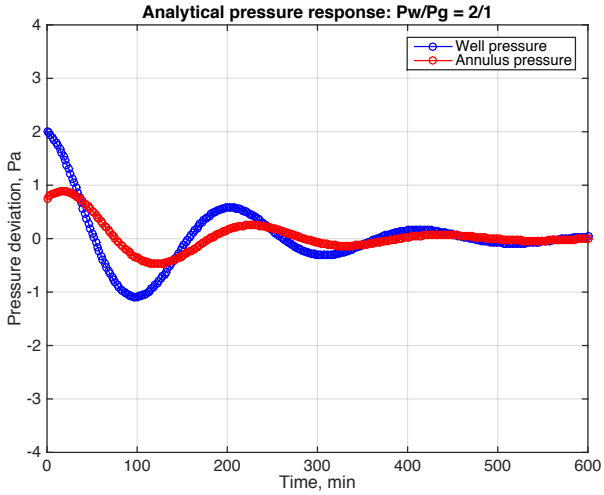

Figure 8.4.2: Analytical pressure response for stable production: $\hat{P}_w$ = 2 Pa, $\hat{P}_g$ = 1 Pa.

8.4.2 Oscillating production

To model oscillating production and to obtain a visually interesting response in the well, the parametric simulation study was initiated using a modified gas lift scenario. Based on this scenario, and by setting the injection rate to $4.85\ 10^4\ Sm^3/d$, the model equation predicted the system to be dynamically unstable.

Figure 8.4.3 shows the response predicted by the analytical solution initiated under the conditions just described. Table 8.4.2 shows the dynamic parameters associated with the solution. Increasing the amplitude ratio seems to increase the attenuation factor while the angular frequency and phase lag decrease.

Table 8.4.2: Dynamic parameters for analytical solution - oscillating production.

$\hat{P_w}/\hat{P_g}$ [-]	Atten.fac. [1/s]	Angular freq. [1/s]	Phase lag [rad/s]
1/1	0.0001	0.0072	-0.8551
2/1	0.0023	0.0015	-0.2588

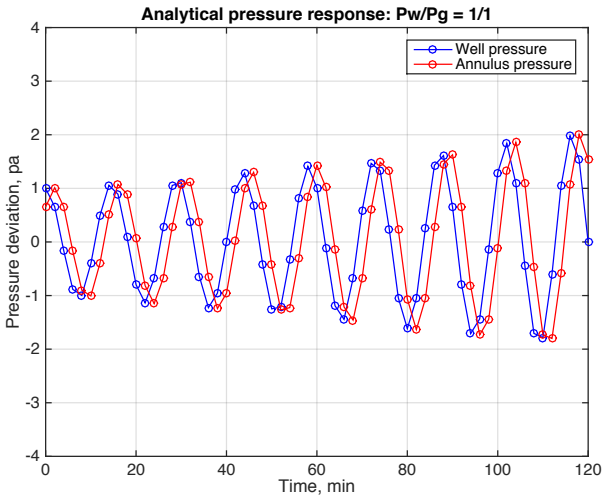

Figure 8.4.3: Analytical pressure response on oscillating production: $\hat{P_w}$ = 1 Pa, $\hat{P_g}$ = 1 Pa.

The result illustrated in figure 8.4.3 is similar to the simulated response in figure 8.3.3. The solution results in positive attenuation factors such that the system may be considered dynamically unstable. We observe that the oscillations increase slowly and thus the analytical solution confirms that the system i undamped. The oscillation period is estimated to 14.4 minutes. Thus, the oscillation period predicted by the analytical solutions is closer to the measured period (8-11 minutes) compared to the oscillation period predicted by simulation.

Figure 8.4.4 shows the response for an amplitude ratio of 2/1. The solution confirms that the system is unstable, but the magnitude of the long-term amplitudes seems to be of no physical meaning. However, it may indicate that the system is further destabilized for higher amplitude ratios.

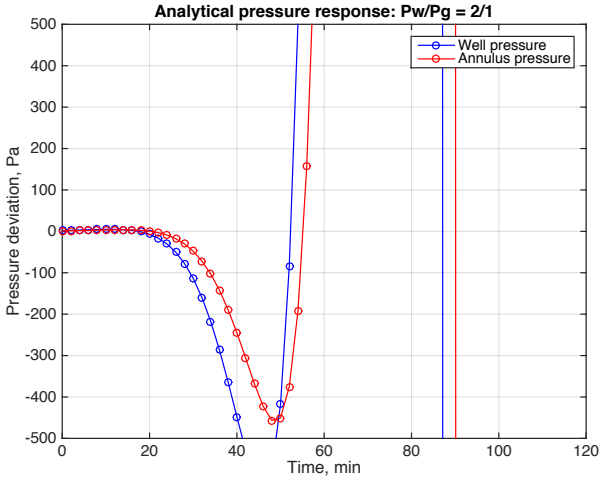

Figure 8.4.4: Analytical pressure response on oscillating production: $\hat{P}_w$ = 1 Pa, $\hat{P}_g$ = 2 Pa.

Chapter 9

Discussion

9.1 Observed characteristics

Analysis of production in the well show pressures and flow rates oscillate severely in certain periods. The months the data were acquired, the measurements reveal the well could maintain stable production only for short periods of time before the production becomes unstable. The oscillations that develop seems to be stable and establishes quickly in the system. They also appear to fluctuate with approximately constant amplitudes and frequencies.

To control production, the field data show Statoil shut-in the well several times. The effect of shutting down production, however, only seems to have a temporary effect on the flow instability.

In the event of stationary production, the analysis shows flow rates are close to perfect normal distributed and that the measurements vary stochastic around the mean. Also, no systematic oscillation frequency is present in the data in the cases of steady production.

9.2 Initiation of instability

The analysis revealed systematic disturbances in the gas delivery system ahead of flow instability. The gas delivery pressure, gas injection pressure, and the gas injection rate all shows variations of the same oscillation periods. The flow instability that later develops in the tubing seems to depend on the characteristics of the disturbances in the gas delivery system. In the event lower frequency variations in the gas delivery system the liquid oscillations that develop have larger amplitudes compared to the case of variations of higher frequency in the gas delivery system. The oscillation periods of the variations in the gas delivery system were estimated to be 12.5 and 13.3 minutes. For an oscillation period of 12.5 minutes, the liquid oscillations that later develop have an amplitude of about 400 Sm^3/d. In the event of an oscillation period of 13.3 minutes, the liquid oscillations have an amplitude of 650 Sm^3/d.

The investigation also identified short lasting and diminishing oscillations in the measurements when the gas delivery system is subjected to small variations with a period of around 24 minutes. This may indicate that the flow in the production tubing is more sensitive to disturbances of higher frequencies, which is more similar to the oscillations that develop in the tubing.

The characteristics of the disturbances imply the gas delivery system oscillate at a lower frequency compared to the oscillations that later develop in the tubing. Although the variations in the gas delivery system are small and have different characteristics, it may have a significant impact on the communication between annulus and tubing. Considering tubing and annulus are connected via the injection valve downhole the conditions in the annulus, and thus the gas delivery system will affect the flow in the tubing. Also, the oscillation period was found similar to the flow time along the production tubing and kinematic waves have been suggested to maybe be one of the reasons for the instability in the well.

9.3 Estimation of static and dynamic parameters from measured data

Both stationary and dynamic parameters have been estimated from the measurements. These estimates depend on the steady-state model's ability to simulate pressure in the well. Estimation of the stationary productivity index involves estimates of the reservoir pressure and flowing bottomhole pressure. The steady-state model use measured production rates and wellhead pressure to estimate the pressure at the bottom of the well. The reservoir pressure was estimated by considering a period of static pressure build-up.

The dynamic productivity index was estimated in certain periods of oscillating production. Using the liquid and the downhole pressure amplitudes gave a dynamic productivity index of around 260 $Sm^3/d/bar$, versus the stationary productivity index of 25 $Sm^3/d/bar$. The magnitude of the dynamic productivity index illustrates the severeness of the oscillations and indicate that the liquid production responds very strongly to the oscillating pressure variations in the well. The liquid amplitudes were estimated to be around 400-650 Sm^3/d while the wellhead and downhole pressure amplitudes were measured to around 7 bars and 2 bars respectively. In periods of unstable production, frequency analysis shows pressures and production rates oscillates at equal frequencies. This indicates the flow instability affect the entire well. The oscillation periods were estimated to be 7.8-10.6 minutes.

The provided field data were acquired using temperature/pressure transducers and multiphase meter, and the accuracy of the measurements will depend on how well calibrated the equipment was. This may affect the estimation of the parameters. The simplifications and

assumptions regarding the steady-state model will also influence the pressure estimates. A more complex model, i.e. including holdup and other flow relations, may give more accurate estimates.

9.4 The dynamic model and dynamic characteristics prediction

Initiated at stationary production, the dynamic model predicts the well dynamically stable for all cases examined. Damped pressure responses like in figure 8.2.1 indicates stability. The simulated response in figure 8.2.2 show that the model can capture the erratic flow behavior observed in the field data. The simulated pressure shows small variations around an average value as seen in the measurements. The response, however, indicates dynamic stability.

Simulation of the model equation depends on initial conditions such that stability prediction by simulation may be misleading, and may give a wrong idea of the dynamics in the well. Therefore, different stationary references have been subjected to various initial disturbances to check the simulation results. Common to all simulations, initiated at field measurements, is that the model predicts the well stable. In certain periods, this is not in agreement with the observed oscillations in the data.

The uncertainties discussed in Chapter 9.3 may also affect the estimation of the response parameters in the dynamic model and thus also the prediction. However, for the model to simulate increasing oscillations the parameters had to be changed rather much. Thus, the accuracy of the measurements is probably not crucial to the disagreement between measured and simulated response.

To model oscillations that increase with time modifications had to be made. The modifications may suggest that the model is particularly sensitive to injection orifice size, gas injection rate, and time delay. When the time delay is estimated from the injection depth to the outlet, the model predicts oscillations that decrease with time. Increased gas injection rate will both reduce the average mixture density and the average flow velocity of the flowing fluid. Reduced flow velocity will increase the time delay in the model. The increase in density will have a big impact on the pressure conditions in the well and thus also the response parameters in the dynamic model. Increasing the diameter of the injection orifice has a significant influence on the inflow of lift-gas to the tubing. This was demonstrated in the sensitivity study.

The sensitivity study illustrates that the model can capture the effect of main design and reservoir parameters on stability. Changing the injection orifice size, gas injection rate, injection depth, and tubing diameter give model responses which correspond well with the literature discussed. The effect of productivity index on the model response, however, does not seem to

coincide with earlier studies. The reason for the disagreement is hard to say and can only be speculated about.

9.5 System versus model

The dynamic gas lift model seems to capture the dynamics observed in the well in certain cases. Initiated at stationary production the model predicts the well stable for all cases. To model unstable production similar to the measurements adjustments had to be made regarding some parameters.

The suggested model seems to encounter a similar problem as existing criteria. In certain production periods, when the model predicts stability the field data show the well was unstable in practice. Although the model considers the variations at the outlet of the tubing, it fails to predict the response in case of oscillating production. However, by including the outflow variations, the model seems to be more sensitive to changes in the reservoir and design parameters. This may be considered as an advance, and a step towards better prediction of stability in gas lifted wells.

It 's hard to give a proper assessment to the difference between the model results and field data. The analysis of the field data revealed an inconsistency regarding provided gas injection pressure and estimated annulus pressure downhole. Thus, there might other errors in the field data that affect the results. It may also be that the instability in the well is due to other factors than what the model takes into account. Another reason to the disagreement may be the simplifications and assumptions in the models.

9.5.1 Further work

Suggestions for further work that may improve the results could be to include slippage, hold-up, and other flow relations in the dynamical model as well as the steady-state model. This may give a more realistic simulation of the conditions in the well.

To verify the model results, it would also be interesting and useful to test the model against another gas lift well that exhibit flow instabilities. In this way, the model's prediction capabilities are checked against independent measurements under other circumstances. Comparing the model results from different cases may be useful considering improvements and updating of the model.

Chapter 10

Conclusion

From the discussion above, the following may be concluded:

- Unstable production in the well exhibits large liquid oscillations with amplitudes of around 400 and 650 Sm^3/d. Pressures and production rates oscillate at equal frequencies and have an oscillation period of about 10 minutes, similar to the flow time along the tubing. Kinematic waves seem likely to be a mechanism of the instability in the well.

- The variations in the gas delivery system also seem likely to be a cause of the instability. Ahead of unstable production, the gas delivery system shows systematic variations with an oscillation period of around 12-13 minutes. The oscillation period seems to influence the size of liquid amplitudes that later develop in the tubing.

- The suggested model seems to improve prediction of flow conditions in certain cases. Initiated at stationary production the dynamic gas lift model predicts the well dynamically stable for all cases examined. The model seems to be able to imitate minor and random variations as observed in the measurements.

- To model oscillations that increase with time modification of the parameters was required. The oscillations simulated by the model equation seems to resemble the characteristics of the measurements to some extent.

- The analytical solution gave results similar to simulation, but the oscillation periods predicted by the analytical solution are closer to the measurements.

- The sensitivity study seems to demonstrate that the model is capable of capturing the effect of main design and reservoir parameters on stability. Excluding the outflow response

appears to reduce the prediction capability of the model.

- The simplifications and assumptions in the models will affect the estimation of the response parameters in the dynamic model and may be a cause of the disagreement between measured and simulated response. It is likely that the accuracy of the field measurements is not a crucial factor to the model results.

Nomenclature

α	attenuation factor, $1/s$
Δt	time delay, s
λ_l, λ_g	flux fractions, $-$
μ_g	gas viscosity, $Pa\ s$
μ_l	liquid viscosity, $Pa\ s$
ω	angular frequency, rad/s
ρ_{fi}	reservoir fluid density at injection point, m^3/kg
ρ_{gi}	lift-gas density at injection point, m^3/kg
ρ_{gsc}	lift-gas density at standard conditions, m^3/kg
ρ_g	lift-gas density, m^3/kg
ρ_l	liquid density, kg/m^3
ρ_m	fluid mixture density, kg/m^3
ρ_{TP}	two-phase fluid mixture density, m^3/kg
$a_1, a_2, b_1, b_2, \epsilon$	grouping of response parameters
A_c	injection port size, m^2
A_g	area occupied by gas phase, m^2
a_g, a_w, c, ft	response parameters
A_l	area occupied by liquid phase, m^2
B_g	gas formation volume factor, m^3/Sm^3
B_o	oil formation volume factor, m^3/Sm^3
C_o	distribution parameter for bubbles in flow, $-$
c_{TP}	slip correction factor, $-$
D	vertical depth to injection valve, m

d tubing diameter, m

E injection orifice efficiency factor, -

F_1, F_2 stability criteria

f_m fluid mixture friction factor, $-$

f_{TP} two-phase friction factor, $-$

g acceleration due to gravity, m/s^2

J productivity index, $Sm^3/d/bar$

J_g gas inflow index at downhole conditions, $m^3/d/bar$

J_w productivity index at downhole conditions, $m^3/d/bar$

L measured depth, m

M_g gas molecular weight, $kg/kmol$

p_g annulus pressure downhole, bar

p_r reservoir pressure, bar

p_{th} tubing head pressure, bar

p_{ti} tubing pressure at injection point, bar

p_{wh} wellhead pressure, bar

q_{fi} flow rate of reservoir fluids at injection point, m^3/d

q_{gi} flow rate of lift-gas at injection point, m^3/d

Q_g gas flow rate at downhole conditions, m^3/d

q_{Lsc} liquid flow rate at standard conditions, Sm^3/d

Q_L liquid flow rate at downhole conditions, m^3/d

R universal gas constant, $J/K/mol$

R_s solution gas-oil ratio, Sm^3/Sm^3

R_t produced gas-oil ratio, Sm^3/Sm^3

T temperature, K

t current time, s

V_c annulus volume, m^3

v_m fluid mixture velocity, m/d

v_o buoyancy velocity of the gas bubbles, or sink velocity for droplets, m/s

v_{sg} gas superficial velocity, m/d

v_{sl} liquid superficial velocity, m/d

V_t tubing volume, m^3

x measured depth to injection point, m

y_l, y_g volume fractions, $-$

References

Alhanati, F., Schmidt, Z., Doty, D., and Lagerlef, D. (1993). Continuous Gas-Lift Instability: Diagnosis, Criteria, and Solutions. *Society of Petroleum Engineers. doi: /10.2118/26554-MS*.

Asheim, H. (1986). MONA, An Accurate Two-Phase Well Flow Model Based on Phase Slippage. *Society of Petroleum Engineers.doi: 10.2118/12989-PA*.

Asheim, H. (1988). Criteria for Gas-Lift Stability. *Society of Petroleum Engineers. doi: 10.2118/16468-PA*, vol 40(11).

Asheim, H. (2000). Analytical Solution of Dynamic Inflow Performance. *Society of Petroleum Engineers. doi: 10.2118/63307-MS*.

Asheim, H. (2016). "11. Gas Lift", Lecture notes, Unpublished, TPG4245 NTNU, URL: http://www.ipt.ntnu.no/ asheim/prodbr.html.

Asheim, H. (2017). Personal communication Spring 2017.

Avest, D. and Oudeman, P. (1995). A Dynamic Simulator to Analyse and Remedy Gas Lift Problems. *Society of Petroleum Engineers. doi: /10.2118/30639-MS*.

Bellarby, J. (2009). *Well Completion Design 1st ed.* Elsevier Science, ISBN-9780444532107.

Bertuzzi, A., Welchon, J., and Poettman, F. (1953). Description and Analysis of an Efficient Continuous-Flow Gas-Lift Installation. *Society of Petroleum Engineers. doi: 10.2118/953271-G*, vol 5(11).

Blick, E., Enga, P., and Lin, P. (1988). Theoretical Stability Analysis of Flowing Oil Wells and Gas-Lift Wells. *Society of Petroleum Engineers. doi: 10.2118/15022-PA*, vol 3(4).

Dalsmo, M. and Halvorsen, E. (2002). Active Feedback Control of Unstable Wells at the Brage Field. *Society of Petroleum Engineers. doi: 10.2118/77650-MS*.

Eikrem, G., Aamo, O., and Foss, B. (2008). On Instability in Gas Lift Wells and Schemes for Stabilization By Automatic Control. *Society of Petroleum Engineers.doi: 10.2118/101502-PA*, vol 23(2).

Fairuzov, Y., Guerrero-Sarabia, C., Carmona-Diaz, R., Cervantes-Baza, T., Miguel-Hernandez, X., and Rojas-Figueroa, A. (2004). Stability Maps for Continuous Gas-Lift Wells: A New Approach to Solving an Old Problem. *Society of Petroleum Engineers. doi: 10.2118/90644-MS*.

Fitremann, J. and Vedrines, P. (1985). Non Steady Gas-Liquid Flow in Pipes and Gas-Lifted Wells. *Conference on Multi-Phase Flow*.

Gang, Z. and Golan, M. (1989). Criteria for Operation Stability of Gas Lift Wells. *Society of Petroleum Engineers*.

Gilbert, W. (1954). Flowing and Gas-Lift Well Performance". Drill. and Prod. Prac. *American Petroleum Institute*.

Grupping, A., Luca, C., and Vermuelen, F. (1984). Heading Action Analyzed for Stabilization. *American Petroleum Institute*, Oil and Gas Journal.

Guerrero-Sarabia, I. and Fairuzov, Y. (2013). Linear and non-linear analysis of flow instability in gas-lift wells. *Journal of Petroleum Science and Engineering. doi: 10.1016/j.petrol.2013.01.012*, vol 108.

Hirch, M. and Smale, S. (1974). *Differential Equations, Dynamical Systems, and Linear Algebra.* Elsevier, ISBN-9780080873763.

Hjalmars, S. (1973). The Origin of Instability in Airlift Pumps. *ASME. J. Appl. Mech. doi:10.1115/1.3422994*, vol 40(2):399–404.

Hu, B. (2004). Characterizing gas-lift instabilities. *Doctoral Thesis NTNU*.

Hu, B. and Golan, M. (2003). Gas-lift Instability Resulted Production Loss and Its Remedy by Feedback Control: Dynamic Simulation Results. *Society of Petroleum Engineers. doi: 10.2118/84917-MS*.

Liu, H. and Vandu, C. (2005). Hydrodynamics of Taylor Flow in Vertical Capillaries: Flow Regimes, Bubble Rise Velocity, Liquid Slug Length, and Pressure Drop. *Ind. Eng. Chem. Res. doi: 10.1021/ie049307n*, vol 44(14).

Myhr, E. (2016). "Gas Lift and Instability", Project report, Unpublished, TPG4560 NTNU.

Norwegian Petroleum Directorate (2017). Heidrun: General information, Retrieved March 4, 2017, from http://factpages.npd.no/ReportServer?/FactPages/PageView/fieldrs:Command=Renderrc:Toolbar=falserc:Parameters=fNpdId=43771IpAddress=129.241.228.11CultureCode=en.

Poblano, E., Camacho, R., and Fairuzov, Y. (2002). Stability Analysis of Continuous-Flow Gas Lift Wells. *Society of Petroleum Engineers. doi: /10.2118/77732-MS*, vol 40(11).

Poettman, F. and Carpenter, P. (1952). The Multiphase Flow of Gas, Oil, and Water Through Vertical Flow Strings with Application to the Design of Gas-lift Installations. *American Petroleum Institute*.

Saepudin, D., Soewono, E., Sidarto, K., Gunawan, A., Siregar, S., and Sukarno, P. (2007). An Investigation on Gas Lift Performance Curve in an Oil-Producing Well. *International Journal of Mathematics and Mathematical Sciences. doi: 10.1155/2007/81519*, vol 07(Article ID 81519).

Slupphaug, O. and Bjune, B. (2006). Active Slug Management. *Society of Petroleum Engineers. doi: 10.2118/96644-MS*.

Appendix A

Steady-state gas lift model

A.1 Model description

The usual way to estimate two-phase steady-state pressure losses is to start with the momentum equation for the mixture in the pipe. Along a pipe segment of length x the following momentum balance has been used.

$$\frac{dp}{dx} + \rho_{TP} g_x + \frac{1}{2} f_{TP} \frac{\rho_{TP}}{d} v_m^2 = 0 \tag{A.1.1}$$

In equation A.1.1, the pressure drop due to acceleration has been neglected. Due to limited information regarding the elevation of the well, the acceleration due to gravity has been normalized considering the relationship between the true vertical depth and measured vertical depth, expressed as g_x.

The brief theory presented in the subsequent sections are included to give the reader an explanation of the functionality of the model and how it simulates pressure and volume rate.

A.1.1 Superficial velocity and mass flow

Considering a pipe segment in the well in which oil, water, and gas flow. At steady-state conditions, the mass flow through any cross section of the pipe is assumed constant. With knowledge of the production rates at surface conditions, the volume streams down in the well can be expressed using the black oil model. In the well, it is convenient to describe the volumes by superficial velocities.

$$v_{sl} = \frac{Q_l}{A_t} = \frac{q_o B_o + q_w B_w}{A_t} \tag{A.1.2}$$

$$v_{sg} = \frac{Q_g}{A_t} = \frac{q_o B_g (R_t - R_s)}{A_t} \tag{A.1.3}$$

The velocity of the mixture are then expressed as the sum of the two individual velocities.

$$v_m = \frac{Q_l + Q_g}{A_t} = v_{sl} + v_{sg} \tag{A.1.4}$$

A.1.2 Fluid velocity, slip and volume fractions

The flow velocity of gas and liquid are linked to the cross-sectional area in the pipe occupied by the two phases. The velocities are defined as the flow rates divided by the cross-sectional area. Expressed in terms of superficial velocities and volume fractions we get.

$$v_l = \frac{Q_l}{A_l} = \frac{\frac{Q_l}{A_t}}{\frac{A_l}{At}} = \frac{v_{sl}}{y_l} \tag{A.1.5}$$

$$v_g = \frac{Q_g}{A_g} = \frac{\frac{Q_g}{A_t}}{\frac{A_g}{At}} = \frac{v_{sg}}{y_g} \tag{A.1.6}$$

Gas will usually flow faster than liquid due to the difference in density and viscosity. Asheim (1986) proposed the following relationship combining the gas velocity to the velocity of the surrounding liquid.

$$v_g = C_o v_l + v_o \tag{A.1.7}$$

Where C_o describes the distribution of bubbles in the flow, and v_o is the buoyancy velocity of the gas bubbles or the sink velocity for the droplets. Asheim (1986) combined the relationship between the superficial velocity and the phase velocity to the drop relationship above, expressing the liquid fraction in the flow as

$$y_l = \pm\frac{1}{2}\sqrt{\left(\frac{v_{sg}}{v_o} + C_o\frac{v_{sl}}{v_o} - 1\right)^2 + 4C_o\frac{v_{sl}}{v_o}} - \frac{1}{2}\left(\frac{v_{sg}}{v_o} + C_o\frac{v_{sl}}{v_o} - 1\right) \tag{A.1.8}$$

The fraction of the gas simply gets

$$y_g = 1 - y_l \tag{A.1.9}$$

Knowing the fluid fractions, the average two-phase density of the fluid mixture in the pipe segment can be expressed in terms of fluid densities and fractions.

$$\rho_{TP} = \frac{\rho_l A_l + \rho_g A_g}{A_t} \tag{A.1.10}$$

A.1.3 Flux fractions and mixed flow

Flux fractions are also linked to superficial velocity and relates flow rate for each phase to the total flowing volume.

$$\lambda_l = \frac{Q_l}{Q_l + Q_g} = \frac{v_{sl}}{v_m} \tag{A.1.11}$$

$$\lambda_g = \frac{Q_g}{Q_l + Q_g} = \frac{v_{sg}}{v_m} \tag{A.1.12}$$

The average mixture density is linked to the flux fractions and is given as

$$\rho_m = \frac{\rho_l Q_l + \rho_g Q_g}{Q_l + Q_g} = \rho_l \lambda_l + \rho_g \lambda_g \tag{A.1.13}$$

The two-phase friction factor, f_{TP}, in equation A.1.1 has been estimated using a correlation for single-phase flow, with a slip correction factor (Asheim, 2016).

$$f_{TP} = f^0 c_{TP} = \frac{0.16}{Re_m^{0.172}} c_{TP} \tag{A.1.14}$$

Where c_{TP} is the slip correction factor and is defined as

$$c_{TP} = \frac{rho_g y_l \left(1 - \lambda_l\right)^2 + \rho_l y_g \lambda l^2}{\rho_m y_l \left(1 - y_l\right)} \tag{A.1.15}$$

The two-phase friction factor has been estimated using the Reynolds Number correlation for a homogeneous flow.

$$Re_m = \frac{\rho_m v_m d_t}{\mu_l \lambda_l + \mu_g \lambda_g} \tag{A.1.16}$$

The theory above form the basis of the steady-state model used in the thesis. The model involves many assumptions and simplifications and is not intended for modeling the flow regimes in the well. The purpose of the model is pressure drop and volume prediction only. The injection of lift-gas down in the well has also been taken into account. At steady-state flow conditions, the model simulates the pressure at the injection point and the bottom of the well. Among several input variables, it uses the pressure at the wellhead and the surface flow rates.

For a given wellhead pressure the model calculates two-phase properties and the pressure at the next step down the well. At the new pressure, two-phase properties are estimated, and the pressure is then recalculated. The procedure is repeated along the tubing down the well until the iteration reaches the perforated section of the well. At the gas injection point, the lift-gas is simply subtracted from the fluid stream to account for the increased gas fraction above the injection valve. This may be observed graphically (7.3.4) by a sudden change of the pressure

gradient in the well. To match the output pressure with the pressure measured in the well, the slip parameters are adjusted.

Appendix B

Dynamic model data

B.1 Response parameters

Table B.1.1 shows the definitions of the response parameters in the model equation and their relations to reservoir and design parameters.

Table B.1.1: Response parameters.

Response parameter	
a_g	$(\rho_l - \rho_g)\,\frac{g_x L}{V_t}\frac{Q_l J_g}{Q_g+Q_l}$
a_w	$\frac{1}{V_t}\frac{(\rho_l-\rho_g)g_x L}{Q_g+Q_l}\left(\frac{A_c^2 Q_l}{\rho_g Q_g} - J_w Q_g\right)$
c	$\frac{p_g}{V_a} J_g$
f_t	$\bar{f_m}\frac{\rho_{\bar{T}} P}{d}\bar{v_m}\frac{L}{A_t}$

B.2 Alternative production reference

Table B.2.1 below summarizes the production conditions for the simulated pressure response in figure 8.2.4.

Table B.2.1: Oscillating production.

Parameter	
Wellhead pressure, [bar]	31.6
Downhole pressure, [bar]	129.9
Bottomhole pressure, [bar]	144.2
Productivity index, $[Sm^3/d/bar]$	25.0
Oil rate, $[Sm^3/d]$	208.7
Water rate, $[Sm^3/d]$	461.2
Gas rate, $[Sm^3/d]$	1.01 10^5
Injection rate, $[Sm^3/d]$	4.73 10^4
Gas injection pressure, [bar]	129.0
Injection orifice diameter, [mm]	11.5

B.3 Production data for sensitivity study

Table B.3.1 summarizes the production data used in the simulations in Chapter 8.3.1.

Table B.3.1: Effect of gas injection rate.

	Injection rate [10^4 $\mathbf{Sm^3/d}$]		
Parameter	**4.85**	**6.85**	**8.85**
Wellhead pressure, [bar]	22.3	22.3	22.3
Downhole pressure, [bar]	129.3	125.0	122.5
Bottom hole pressure, [bar]	145.7	141.2	138.2
Oil rate, [Sm^3/d]	203.8	239.6	263.3
Water rate, [Sm^3/d]	430.1	505.5	556.6
Gas rate, [Sm^3/d]	8.68 10^4	1.13 10^5	1.38 10^5

Table B.3.2 summarizes the production data used in the simulations in Chapter 8.3.3.

Table B.3.2: Effect of productivity index.

	Productivity index [$\mathbf{Sm^3/d/bar}$]		
Parameter	**5.0**	**25.0**	**45.0**
Wellhead pressure, [bar]	22.3	22.3	22.3
Downhole pressure, [bar]	129.3	122.5	131.9
Bottom hole pressure, [bar]	108.9	138.2	148.2
Oil rate, [Sm^3/d]	99.9	263.3	328.0
Water rate, [Sm^3/d]	210.7	556.1	692.2
Gas rate, [Sm^3/d]	1.07 10^5	1.38 10^5	1.50 10^5